Breakthrough report

Gametophytic epigenetic regulators MEA and DME synergistically suppress ectopic shoot formation in *Arabidopsis*

Mohit Rajabhoj[1], Sudev Sankar[1,3], Ramesh Bondada[1,4], Anju P Shanmukhan[2], Kalika Prasad[2]*, Ravi Maruthachalam[1]*

[1]*School of Biology, IISER-Thiruvananthapuram, Trivandrum, Kerala 695551, India*
[2]*Department of Biology, IISER-Pune, Pune, Maharashtra 411008, India*
[3]*Present address: Department of Plant and Microbial Biology & Zurich-Basel Plant Science Center, University of Zurich, Zollikerstrasse 107, Zurich 8008, Switzerland*
[4]*Present address: Department of Biology and Gus R. Douglass Institute, West Virginia State University, WV 25112-1000, USA*
*Corresponding authors: ravi@iisertvm.ac.in, kalika.prasad@iiserpune.ac.in

Keywords: MEDEA, DEMETER, shoot development, epigenetics, histone methylation, DNA methylation

Running title: MEA and DME control shoot development

Abstract

The gametophyte to sporophyte transition is an important event facilitating the alternation of generations in a plant life cycle. The paternally imprinted epigenetic regulators DEMETER(DME) and MEDEA(MEA) synergistically control central cell proliferation and differentiation, ensuring proper gametophyte to sporophyte transition in *Arabidopsis*. Mutant alleles of *DME* and *MEA* are maternal lethal, eluding the recovery of recessive homozygotes to examine their role in the sporophyte. Here, we exploited the paternal transmission of these mutant alleles coupled with CENH3-haploid inducer to generate *mea*-1;*dme*-2 sporophytes. Strikingly, the simultaneous loss of function of MEA and DME leads to the emergence of multiple shoot meristems at the apical pole of the plant body axis. *DME* and *MEA* are expressed in the developing shoot apex and regulate the expression of various shoot-promoting factors. Chromatin immunoprecipitation(ChIP) and DNA methylation analysis revealed several shoot regulators as potential targets of MEA and DME, with *mea*-1$^{-/-}$;*dme*-2$^{-/-}$ seedlings showcasing their misexpression. Knockdown of upregulated shoot-promoting factors STM, CUC2, and PLT5 rescued the ectopic shoot phenotypes. Our findings reveal a previously unrecognized synergistic role of MEA and DME in restricting the meristematic activity at the shoot apex during sporophytic development to orchestrate the plant architecture.

Introduction

Sporophyte development in higher plants results from a fine balance between cell growth and differentiation at the meristems. Primary meristems at the shoot and root apices are responsible for all post-embryonic organ development, coordinated by the polar gradients of plant hormones (Stahl and Simon, 2010; Ten Hove *et al*., 2015). Throughout this process, epigenetic regulatory complexes provide an additional fine-tuning of gene expression, further contributing to plant developmental plasticity. Regulators of Histone methylation like Polycomb repressive complex 1 & 2 (PRC1 & PRC2) transcriptionally repress embryonic regulators such as *BABYBOOM* (*BBM*),

LEAFY COTYLEDON1 & *2* (*LEC1* & *LEC2*) (Chen *et al*., 2010). In contrast, the EMBRYONIC FLOWER (EMF)- and VERNALIZATION (VRN)-PRC2s regulate sporophyte development during the transition from the vegetative to the reproductive life phase (Yoshida *et al*., 2001; De Lucia *et al*., 2008). Genes expressed during shoot development like *WUSCHEL* (*WUS*), *SHOOT MERISTEMLESS* (*STM*), *AGAMOUS* (*AG*), *BREVIPEDICELLUS* (*BP*), *KNOTTED-LIKE FROM ARABIDOPSIS THALIANA 2* (*KNAT2*), and *KNUCKLES* (*KNU*) are known targets of PRC2 components, and their expression domain is instructed by trimethylation of histone H3 at Lys27 (H3K27me3) repression mark (Kwon *et al*., 2006; Lodha *et al*., 2013; Sun *et al*., 2019; Xiao and Wagner, 2015; Xiao *et al*., 2017). *PLETHORA* (*PLT*) transcription factors are known for regulating lateral organ initiation at both the root and shoot apices (Prasad *et al*., 2011; Hofhuis *et al*., 2013). Although auxin gradients mainly regulate the PLT expression domains, the root meristem-specific PLTs are also epigenetically regulated (Aichinger *et al*., 2011; Lee and Seo, 2018). *PLTs*, in turn, control the shoot-promoting gene family *CUP-SHAPED COTYLEDON* (*CUC*) (Kareem *et al*., 2015). CUCs and STM positively regulate each other to maintain stem cell populations and promote organ formation at the shoot apical meristem (SAM) boundary (Spinelli *et al*., 2011). CUCs are also positively regulated by chromatin remodeling factors like BRAHMA (BRM), which is required to establish leaf primordia (Shen and Xu, 2009). These reports indicate the maintenance of a delicate balance of CUCs expression during shoot development *via* direct or indirect epigenetic regulators. Apart from controlling shoot development, epigenetic marks such as H3K27me3 and DNA methylation are often reset during major developmental phase transitions, such as gamete and embryo formation (Slotkin *et al*., 2009; Iwasaki and Paszkowski, 2014; Borg *et al*., 2020). Such a reset helps demarcate embryonic and meristematic programs in growing shoots while maintaining a pool of undifferentiated cells at the meristem (Kuwabara and Gruissem, 2014; Pikaard and Scheid, 2014).

An epigenetic reset essential for normal embryo development in *Arabidopsis thaliana* is mediated by the components of FERTILIZATION INDEPENDENT SEED-Polycomb Repressive Complex 2 (FIS-PRC2) and DNA glycosylase DEMETER (DME) (Xiao *et al*., 2003; Gehring *et al*., 2006). DME and members of FIS-PRC2 complex like MEDEA (MEA) are primarily expressed in central cells of the embryo sac (Choi *et al*., 2002; Luo *et al*., 2000). The loss-of-function mutations in these

genes result in female gametophyte lethality reflected as parent-of-origin defects during seed development. DME and MEA are known to regulate seed development together, where DME activates the expression of MEA in the central cell by removing DNA methylation marks from *MEA* promoter and intergenic regions (Xiao *et al*., 2003; Gehring *et al*., 2006). Apart from gametogenesis and seed development, histone methylation mediated by FIS-PRC2 also shapes seedling transitions by modulating seed dormancy and repression of embryonic traits in developing seedlings (Bouyer *et al*., 2011).

Similarly, DNA methylation is reported to be high in developing seedlings to suppress transposon element expression and maintain an undifferentiated stem cell niche (Bouyer *et al*., 2017; Higo *et al*., 2020). These reports indicate the vital role of DNA and histone methylation in shaping plant architecture, with PRC2 members like MEA and DNA glycosylases like DME likely to participate in transcriptional regulation. Thus, a complete loss-of-function of DME and MEA provides an ideal system for examining their function during sporophytic development.

Mutant alleles of *DME* and *MEA* are transmitted through male gamete as microsporogenesis and microgametogenesis proceeds unhampered in most such mutants, but not through female lineage (Grossniklaus *et al*., 1998; Choi *et al*., 2002; Köhler *et al*., 2003). The generation of homozygous gametophytic lethal mutants thus is challenged by conventional genetic approaches, which rely on self-pollination and inbreeding of heterozygous single/double mutants to generate respective homozygotes barring those alleles with the leaky transmission. Hence, it is difficult to decipher the role of such gametophyte-lethal genes, if any, in sporophytic development. Studies involving maternal lethals of *DME*, *MEA,* and their epigenetic regulation in sporophytes thus relied either on examining heterozygotes (Roszak and Köhler, 2011; Schoft *et al*., 2011; Figueiredo *et al*., 2015; Park *et al*., 2017; Zhang *et al*., 2018; Khouider *et al*., 2021) or homozygous plants carrying a weak allele (Park *et al*., 2017; Kim *et al*., 2021; Simonini *et al*., 2021; Williams *et al*., 2022), thereby restricting complete understanding of their function. Alternate methods to study DME and MEA in sporophyte development have been used previously, including paternal haploids from single mutants, conditional homozygotes, and homozygotic progeny of transheterozygote mutants (Ravi *et al*., 2014; Roy *et al*., 2018; Simonini *et al*., 2021;

Kim *et al*., 2021). The extended roles of MEA and DME in sporophytes deciphered using *mea* and *dme* single mutants prompted us to generate and investigate the sporophytic phenotypes of *mea*; *dme* double homozygotes.

Here, we employed haploid genetics to generate viable *mea* $^{-/-}$;*dme* $^{-/-}$ doubled haploid (DH) sporophytes. Using these DH mutant homozygotes, we show that MEA and DME are essential for the later sporophyte development of *Arabidopsis thaliana* plants. Loss of function of MEA and DME leads to the emergence of more than one functional shoot meristem at the apical pole of the plant body axis. We further show that these epigenetic regulators control the shoot meristem development by regulating key shoot-promoting factors such as *STM*, *PLT5*, and *CUC2*. Our studies reveal a new role of MEA and DME mediated epigenetic regulation in controlling shoot architecture during post-embryonic development.

Results

mea-1$^{-/-}$;*dme*-2$^{-/-}$ double mutants are viable and initiate functional ectopic SAM

Previous studies have established that MEA and DME play a key role in seed development by regulating polar nuclei and endosperm division after double fertilization (Grossniklaus *et al*. 1998; Choi *et al*. 2002). Several *dme* and *mea* alleles have been isolated by induced mutagenesis from some select natural *Arabidopsis thaliana* accessions (Choi *et al*. 2002; Guitton *et al*. 2004; Schoft *et al*. 2011). Irrespective of the accession, both *dme* and *mea* mutant alleles can be transmitted through pollen (male) with rare or no maternal female transmission resulting in >25% seed lethality upon self-fertilization of the corresponding heterozygotes. We have earlier shown that generating *mea* and *dme* paternal haploid plants is possible using CenH3-mediated haploid induction (Ravi *et al*., 2014; Roy *et al.*, 2018). Here, we advanced further to generate doubled haploid(DH) plants of *dme*-2$^{-/-}$ (L*er*), *dme*-6$^{-/-}$, *dme*-7$^{-/-}$ (Col-0), and *mea*-1$^{-/-}$ (L*er*), *mea*-6$^{-/-}$, *mea*-7$^{-/-}$ (C24) mutants to examine the recessive vegetative phenotypes associated with *dme* and *mea* mutants (Figure 1A, Supplementary Table 1). Here, we used *dme*-2 and *mea*-1 alleles for generating double homozygotes for the following reasons; firstly, among all the mutant alleles characterized, *mea*-1 and *dme*-2 are reported to show strong loss-of-function phenotypes (Grossniklaus *et al*., 1998; Choi *et al*., 2002; Simonini *et al*., 2021; Kim *et al*., 2021),

153 which is ideal for double mutant studies. Secondly, both alleles are of the Landsberg
154 *erecta* (L*er*) ecotype, which yields a high number of spontaneous DH seeds than Co-
155 lumbia (Col-0) (Ravi and Chan, 2010). This feature is essential to maximize seed
156 yield to obtain viable spontaneous doubled haploid seeds in the strong gametophyte
157 lethal alleles with high seed abortion like *mea*-1 and *dme*-2. Thirdly, identical L*er*
158 backgrounds of single mutants of *mea* and *dme* ensure genetic homogeneity in the
159 resultant double mutants, thereby avoiding confounding effects due to different ge-
160 netic backgrounds.

161 *mea*-1 haploids, when germinated in Murashige and Skoog agar (MSA) plates,
162 showed no visible phenotypic defects and grew normal as that of their wild-type sib-
163 lings. *mea*-1 haploids produced a good number of spontaneous DH seeds, of which
164 2% (n= 21/1178, pooled from 14 haploid plants) were viable, giving rise to *mea*-1$^{-/-}$
165 DH offspring. Most seeds produced by DH *mea*-1$^{-/-}$ plants were atrophied (81%, n=
166 1407/1754, supplementary figure 1) in confirmation with previous reports (Simonini
167 *et al*., 2021). A small fraction of germinated seedlings (4%, n= 14/338) failed to grow
168 beyond the cotyledonary leaf stage and perished two to four days post-germination
169 (dpg). Unlike *mea*-1 haploids, a fraction of *mea*-1$^{-/-}$ (33%, n= 107/324) displayed
170 stunted and aberrant vegetative growth (Supplementary Figure 2). However, when
171 transferred to the soil medium, these seedlings recovered and showed normal vege-
172 tative growth with no discernible phenotypes.

173 Like *mea*-1 haploids, *dme*-2 haploids also showed normal vegetative growth but se-
174 vere seed abortion during reproductive development (98%, n= 1286/1308), owing to
175 the strong loss-of-function of *dme*-2. Spontaneous *dme*-2$^{-/-}$ DH seeds harvested from
176 *dme*-2 haploid plants showed less than 2% (n= 22/1308) germination on the MSA
177 medium. About 10% (n= 43/478) of *dme*-2$^{-/-}$ seedlings ceased to grow beyond the
178 cotyledon leaf stage (Supplementary Figure 1D). Unlike *mea*-1$^{-/-}$ seedlings, a vast
179 majority of *dme*-2$^{-/-}$ seedlings (78%; n= 341/435) exhibited developmental abnormali-
180 ties such as fused cotyledons, delayed emergence of true leaves, stunted hypocotyl,
181 and retarded root growth (Supplementary Figure 2). Despite these abnormalities,
182 most of the *dme*-2$^{-/-}$ seedlings (n= 153/157) recovered from the early vegetative
183 growth defects when they transitioned to the adult stage, similar to that observed for
184 *mea*-1$^{-/-}$ homozygotes. However, unlike *mea*-1$^{-/-}$ plants, *dme*-2$^{-/-}$ plants displayed flo-

ral defects like improper petal number and positioning, and abnormalities in gynoecium, as reported in earlier studies (Supplementary Figure 3, Ravi *et al*., 2014; Kim *et al*., 2021).

Next, we attempted to generate *mea*-1$^{-/-}$;*dme*-2$^{-/-}$ double homozygotes to examine the loss of histone methylation (H3K27me3) and DNA demethylation mediated by MEA and DME, respectively, during early vegetative development of seedlings. To this end, we crossed *mea*-1$^{+/-}$;*dme*-2$^{+/-}$ as a pollen parent, with haploid inducer GFP-*tailswap* as female, and selected *mea*-1;*dme*-2 haploids(n=9/32) by PCR-based genotyping (Figure 1A, Supplementary Figure 1).

The spontaneous DH seeds obtained from *mea*-1;*dme*-2 haploid plants showed less than 1% (n= 13/1950) viability up to germination (Supplementary Figure 1). The *mea*-1;*dme*-2 haploids showed normal vegetative development as that of *mea*-1 and *dme*-2 haploids. The *mea*-1$^{-/-}$;*dme*-2$^{-/-}$ offspring were grown further for bulk seed production. The selfed *mea*-1$^{-/-}$;*dme*-2$^{-/-}$ plants continued to produce atrophied seeds (n= 1678/1681), as observed in the parent generation. Around 38% (n= 87/226) of germinated *mea*-1$^{-/-}$;*dme*-2$^{-/-}$ were arrested in development and displayed pale and fused cotyledons (Supplementary Figure 2). The remaining viable *mea*-1$^{-/-}$;*dme*-2$^{-/-}$ seedlings displayed severely stunted growth and shorter hypocotyl compared to wild-type (Figure 1B). Such seedlings also showed underdeveloped and fused cotyledons without petioles compared to WT (Figure 1C-E). We also observed smaller, asymmetric true leaves, indicating defects during shoot development (n= 107/139). Also, nearly half the number of *mea*-1$^{-/-}$;*dme*-2$^{-/-}$ seedlings (n= 71/139) displayed ectopic shoot emerging from the existing shoot apex (Figure 1F, G). Further microscopic analysis of such *mea*-1$^{-/-}$;*dme*-2$^{-/-}$ plants shoot apices revealed the presence of two SAMs consistent with the presence of ectopic shoots (n= 25/48). Figure 1L, M). Like *mea*-1$^{-/-}$ and *dme*-2$^{-/-}$ single mutant plants, *mea*-1$^{-/-}$;*dme*-2$^{-/-}$ plants also recovered from their early developmental defects and displayed normal vegetative growth in the later stages (n= 129/132, Figure 1I, Supplementary Figure 3). In *mea*-1$^{-/-}$;*dme*-2$^{-/-}$ plants with ectopic shoot, both SAMs developed independently, which upon vegetative to reproductive transition, gave rise to two inflorescence shoots from a single vegetative body (rosette) (Figure 1I, K, Supplementary Figure 3). This “twin-plant” phenotype is reminiscent of conjoined twins having two independent upper trunks

with a common lower portion of the body. The “twin plant” phenotype arising from persistent ectopic shoots suggests a role for DME and MEA in regulating shoot meristematic activity, as reported previously (Kim *et al*. 2021; Simonini *et al*. 2021).

Interestingly, we note that a fraction of single mutant *mea*-1, *dme*-2, and *mea*-1;*dme*-2 double mutants show no visible developmental defects and display WT phenotype. Even single and double mutant seedlings that show early developmental defects post-germination show resilience at later stages of vegetative development. However, the ectopic shoots initiated during early developmental stages persist throughout the plant life cycle, displaying twin plant phenotype. This observation suggests that the function of both DME and MEA is predominantly required only during juvenile growth but dispensable for later vegetative growth.

MEA and DME are expressed in developing shoot meristems and leaf primordia

To decipher if the aberrant vegetative phenotypes in *mea*-1$^{-/-}$;*dme*-2$^{-/-}$ seedlings result from the loss-of-function of MEA and DME, we sought to examine their expression patterns of *MEA* and *DME* in germinated seedlings. Recent reports have shown that in addition to its gametophyte expression in the central cell of the female gametophyte and sperm cells of the pollen, *DME* is also expressed in sporophytic tissues such as the developing SAMs, root apical meristems (RAMs) and inflorescence meristems (IMs) (Kim *et al*., 2008; Park *et al*., 2017). Likewise, *MEA* is expressed in the developing embryo till the torpedo stage (Vielle-Calzada *et al*., 1999; Spillane *et al*., 2007) and induced in sporophytic tissues on demand when challenged with pathogens (Roy *et al*., 2018). Further, transcriptome data also indicates the expression of MEA and DME mRNA in the seedlings and other sporophytic tissues (Schmid *et al*., 2005). Besides these reports, a systematic expression analysis of *DME* and *MEA* during early seedling development needs to be improved. The ectopic shoot phenotype in *mea*-1$^{-/-}$;*dme*-2$^{-/-}$ seedlings prompted us to examine the detailed expression pattern of MEA and DME in early seedlings. Hence, we first attempted real-time PCR to examine the transcript levels of *MEA* and *DME* mRNA. For this, we extracted total RNA from 1, 3, 5, 7, and 10-day-old seedlings, respectively, from *mea*-1$^{-/-}$;*dme*-2$^{-/-}$ and wild-type (WT) seedlings as control. Here, we found high

expression of *DME* mRNA until 2 dpg, with a decline in expression after 3 dpg. *DME* mRNA expression again increases after 5 dpg with plant growth (Figure 2A). On the other hand, we observed *MEA* mRNA expression to be low in the early stage of vegetative development but steadily increased over time till the 10 dpg seedling stage.

Next, we examined the spatiotemporal expression pattern of DME and MEA during early sporophytic growth by confocal microscopy of the WT embryos and seedlings expressing *pMEA*::*gMEA*:*vYFP* and *pDME*::*gDME*:*vYFP* translational fusions. Both, *pMEA*::*gMEA*:*vYFP* and *pDME*::*gDME*:*vYFP* transgenes were functional and rescued the *mea*-1 $^{-/-}$ and *dme*-2 $^{-/-}$ mutant phenotypes (Supplementary Figure 4, Supplementary Table T1). The rescue in seed lethality and expression pattern suggests that both the transgenes harbor necessary cis-regulatory sequences capable of recapitulating the endogenous expression pattern of *MEA* and *DME*. We further monitored the expression patterns of *MEA* and *DME* using *pMEA*::3X-*VENUS* and *pDME*::3X-*VENUS* in developing embryos and shoots (Supplementary Figure 4). Consistent with the previous studies, we observed active *MEA* transcription in developing embryos (Vielle-Calzada *et al*.,1999; Spillane *et al*., 2007). *pMEA-driven* VENUS reporter is visible until the globular stage embryo, with scattered expression observed in the later embryonic stages (n= 33/45) (Figure 2B-F). On the other hand, we observed *DME* was observed to be expressed in all developmental stages of the embryo, i.e., from the four-celled to the walking-stick stage embryos (n= 66/71) (Figure 2G-K).

We further examined the expression pattern of *MEA* and *DME* in the shoot apex. Previous studies have documented the expression of *DME* in developing leaves of seedlings (Kim *et al*., 2008; Park *et al*., 2017; Jullien *et al*., 2008). However, it is unclear from these studies where MEA and *DME* are expressed in the shoot meristem. We, therefore, examined the expression patterns in shoot meristem during post-embryonic development. *MEA* was predominantly expressed in the peripheral domain of the shoot meristem (Figure 2L). Its expression was also detected in developing leaf primordia (Figure 2M). As reported earlier, *DME* was expressed uniformly throughout the shoot meristem (Figure 2N) (Kim *et al*., 2008; Park *et al*., 2017). Like *MEA*, its expression was also detected in developing leaf primordia (Figure 2O).

Taken together, the expression patterns of *MEA* and *DME* corroborate their role in maintaining shoot meristems.

MEA and DME repress the expression of shoot-promoting factors

We next examined if the ectopic shoot meristems in *mea*-1$^{-/-}$;*dme*-2$^{-/-}$ make functional stem cell niches. Toward this, we examined the expression *pWUS*::3X-*VENUS*:*tWUS.* WUS is a marker for SAM stem cell niche (Mayer *et al*., 1998; Schoof *et al*., 2000; Yadav *et al*., 2013). Strikingly, *mea*-1$^{-/-}$;*dme*-2$^{-/-}$ seedlings showed ectopic *WUS* promoter activity at the shoot apex (n= 21/48, Figure 3G, G(i) to G (iii)) as compared to WT seedlings where WUS-YFP is confined to one organizing center (Figure 3F). Ectopic WUS-YFP corroborates with shoot phenotype seen in *mea*-1$^{-/-}$;*dme*-2$^{-/-}$. We also observed ectopic WUS-YFP activity in developing cotyledons of *mea*-1$^{-/-}$;*dme*-2$^{-/-}$ embryos and SAM (n= 26/78) (Figure 3D-E). This indicates de novo organizing centers specified in the non-canonical regions in the embryos, as reported earlier (Simonini *et al*., 2021).

We next examined the expression of genes essential for lateral organ initiation. PIN1 expression is an indicator of auxin transport whose expression is instrumental in organ initiation in the actively dividing SAM (Heisler *et al*., 2005). PIN1-GFP was detected in shoot meristem and in developing leaf primordia of ectopic shoots of *mea*-1$^{-/-}$;*dme*-2$^{-/-}$ mutant (n=29/55, Figure 3U). Ectopic transport of auxin suggests ectopic initiation of aerial organs in SAM. As expected, PIN1-GFP was expressed in wild-type and mutant embryos (Figure 3H-S). Similar to WUS, we found ectopic PIN1 expression in the mutant embryos (Figure 3L-S).

We further analyzed the expression of genes that regulate the boundary between the meristem and developing lateral organ primordia. The transcription factor, CUC2, is an early marker of shoot organ boundary specification at SAM (Heisler *et al*., 2005). CUC2 expression in developing embryo displays characteristic stripe formation in the central domain away from protoderm cells till the heart shape stage but later surrounds the SAM between its boundary with cotyledons (Aida *et al*., 1999; Aida *et al*., 2002) (Figure 3V, W). For *pCUC2*::*CUC2*:*vYFP*; *mea*-1$^{-/-}$;*dme*-2$^{-/-}$ embryos, the typical stripe pattern of CUC2-vYFP in the central domain is lost, and we observed more dispersed expression in SAM initial and protoderm cells (n= 31/77). (Figure 3Z, A').

311 In a few embryos, we observed CUC2-vYFP expression in the cotyledon, defining a
312 new region for organ initiation compared to wild-type (n=15/77) (Figure 3B', C').
313 Similarly, CUC2-vYFP expression in *mea*-1$^{-/-}$;*dme*-2$^{-/-}$ shoots is dispersed along the
314 peripheral and central zone instead of being restricted at the organ primordia (Figure
315 3E'). The ectopic expression of CUC2-vYFP indicates the de-repression of *CUC2* in
316 SAM, which is essential for proper organ initiation and patterning (Burian *et al*.,
317 2015). Corroborating with the mutant phenotype, we also observed an increase in
318 the transcript levels of a variety of shoot regulators such as
319 *CUC2*, *CUC3*, *YUC4*, *PLT5, STM*, *KNAT1*, and *KNAT6* in *mea*-1$^{-/-}$;*dme*-2$^{-/-}$ seedlings
320 (Figure 3A). These data demonstrate the de-repression of most canonical shoot reg-
321 ulators in *mea*-1$^{-/-}$;*dme*-2$^{-/-}$ seedlings.

322 **Shoot regulators are targets of MEA and DME during early shoot development**

323 The ectopic shoot phenotype in *mea*-1$^{-/-}$;*dme*-2$^{-/-}$ plants, coupled with the expression
324 of *DME* and *MEA* in the early sporophyte, prompted us to identify critical targets of
325 MEA and DME that regulate the shoot meristem specification. The interplay between
326 DNA methylation and histone modifications in specifying cell fate and differentiation
327 during development is well-known in animals and plants (Du *et al*., 2015; Williams
328 and Gehring, 2020). For instance, a positive feedback loop between DNA methyla-
329 tion and H3K9 methylation maintains the heterochromatin in a repressed state in
330 plants (Du *et al.*, 2015). H3K27 methylation, similarly, has been observed predomi-
331 nantly in the heterochromatin state associated with non-CG methylation. The prefer-
332 ential binding of the histone demethylase RELATIVE OF EARLY FLOWERING 6
333 (REF6) to hypo-methylated DNA leads to the loss of the H3K27me3 mark from the
334 chromatin (Cui *et al.*, 2016; Qiu *et al.*, 2019). Hence, we hypothesized that a similar
335 interaction between DNA methylation and histone methylation could be jointly medi-
336 ated by the action of DME and MEA, leading to the regulation of the shoot regula-
337 tors.

338 As a histone methyltransferase, MEA catalyzes the trimethylation of H3K27. Hence,
339 to identify targets of MEA, we performed whole genome profiling of H3K27me3 lev-
340 els by Chromatin Immunoprecipitation (ChIP)-seq experiment. Here, we observed
341 4994 significant peaks in WT compared to *mea*-1$^{-/-}$;*dme*-2$^{-/-}$ seedlings. Out of anno-
342 tated 3885 H3K27me3 binding loci, we selected 431 enriched gene loci for further

343 analysis based on their role in shoot development as predicted by the Gene Ontolo-
344 gy Resource (http://geneontology.org/)(Figure 4A). These 431 genes encompass
345 known shoot regulators like *STM*, *KNAT1*, *CUC2*, *PLT5*, *ESR1* & *2*, *CKX3*, *AHP6*,
346 *KNU*, and *YUC4*. Upon closer examination, we found H3K27me3 binding more per-
347 sistent in the promoter region (90.4%) of these genes, as reported by earlier studies
348 (Zhang *et al*., 2007; Xiao *et al*., 2016). We also observed differential H3K27me3
349 binding in the gene body region of *CUC2*, *PLT5*, *STM*, and *WUS* (Figure 4B-E). This
350 loss of repressive H3K27me3 mark in *mea*-1$^{-/-}$;*dme*-2$^{-/-}$ for such genes predicts ac-
351 tive and ectopic transcription. We next examined the expression levels of potential
352 shoot regulators identified genome-wide in *mea*-1$^{-/-}$;*dme*-2$^{-/-}$ mutant seedlings by RT-
353 qPCR. Regulators of organ initiation, like *CUC3*, *YUC4*, and *ESR2,* were upregulat-
354 ed in the mutant seedlings compared to WT plants (Figure 4A). Similarly, genes in-
355 volved in stem cell maintenance, like *STM*, *KNAT1*, and *KNAT6*, were upregulated
356 compared to WT (Figure 4A). Overall, we see a de-repression of various shoot regu-
357 lators in *mea*-1$^{-/-}$;*dme*-2$^{-/-}$ seedlings. This observation is consistent with the loss of
358 repressive H3K27me3 mark in *mea*-1$^{-/-}$;*dme*-2$^{-/-}$ plants (Figure 3A).

359 To identify the likely targets of DME, we carried out Chop PCR for particular genes
360 that affect shoot development (Zhang *et al*., 2014). Chop-PCR employs methylation-
361 sensitive restriction enzymes (MSRE) to differentially digest methylated and un-
362 methylated DNA, followed by PCR of the digested product. Here, we used McrBC,
363 which recognizes at least two methylated cytosines, preceded by purines: A or G, in
364 the range of 40-3000 bp to cleave 30bp aside of methylated cytosine (Sutherland *et*
365 *al*., 1992). Therefore, a heavily methylated DNA region will be less amplified upon
366 McrBC-digested chop-PCR (Dasgupta and Chaudhari, 2019). We chose upstream
367 regions of genes like *WUS* and *STM* for Chop-PCR. Based on available methylome
368 data (1001 Genome Project; http://neomorph.salk.edu/1001.aj.php) and their known
369 role in shoot development, we examined their DNA methylation pattern in *mea*-1 $^{-/-}$
370 ;*dme*-2 $^{-/-}$ seedlings. We identified DNA methylation patches in the upstream region
371 of both genes and designed gene-specific oligonucleotides to amplify those regions after
372 McrBC digestion (Figure 4F, G). We observed weak amplification
373 for *WUS* and *STM* promoter regions in *mea*-1$^{-/-}$;*dme*-2$^{-/-}$ seedlings, indicating methyl-
374 ated DNA region (Figure 4H). Change in DNA methylation pattern may be associat-

375 ed with the differential expression pattern of these genes in the *mea*-1$^{-/-}$;*dme*-2$^{-/-}$ de-
376 veloping seedlings.

377 **Downregulation of shoot regulators in *mea*-1 $^{-/-}$;*dme*-2 $^{-/-}$ leads to a partial res-**
378 **cue of the ectopic shoot phenotype**

379 Since the majority of shoot regulators are over-expressed in the SAM of *mea*-1$^{-/-}$
380 *;dme*-2 $^{-/-}$ seedlings, we sought if down-regulation of select shoot regulators viz.,
381 STM, PLT5, and CUC2 would suppress the ectopic shoot formation. Our selection of
382 these genes for further analysis is based on previously implicated role in promoting
383 the shoot meristem formation. While CUC2 and STM were earlier shown to be suffi-
384 cient for ectopic shoot meristem initiation (Daimon *et al*., 2003; Scofield *et al*., 2008),
385 we found inducible PLT5 over-expression sufficient for triggering ectopic cell prolifer-
386 ation in the shoot (Supplementary Figure 6).To examine the consequence of down-
387 regulating STM, PLT5, and CUC2 in the *mea*-1$^{-/-}$*;dme*-2$^{-/-}$, we performed estradiol-
388 inducible RNAi-mediated gene silencing. Upon estradiol-induced RNAi, *STM*
389 *mRNA* levels reduced from 5.42 fold to 0.71 fold in *STM-dsRNAi*; *mea*-1$^{-/-}$*;dme*-2$^{-/-}$
390 seedlings vs. WT seedlings (Figure 5A). Similarly, *CUC2-dsRNAi* and *PLT5-*
391 *dsRNAi* constructs decreased *CUC2* and *PLT5 mRNA* levels from 2.52 and 3.54 fold
392 to 0.93 and 0.6 fold, respectively (Figure 5A). The reduction in mRNA levels
393 of *STM*, *CUC2*, and *PLT5* correlated with the reduction of ectopic shoots in *mea*-1$^{-/-}$
394 *;dme*-2$^{-/-}$ plants (Figure 5B). Here, estradiol-induced downregulation of *STM* in *mea-*
395 1$^{-/-}$*;dme*-2$^{-/-}$ germinating seedlings reduced the frequency of ectopic shoot from 49%
396 (N=4, n= 68/139, uninduced mock-treated seedlings) to 9% (N=4, n= 9/98, estradiol-
397 induced seedlings), suggesting a partial rescue to WT phenotype (N=4, n= 89/98,
398 Figure 5B, C). Similarly, RNAi-mediated knock-down of *CUC2* and *PLT5*
399 *mRNA* in *mea*-1$^{-/-}$*;dme*-2$^{-/-}$ germinating seedlings resulted in the reduction of ectopic
400 shoots to 23% (N=3, n= 32/134) and 12% (N=4, n= 28/231), respectively (Figure 5B,
401 Supplementary Figure 5). We interpret the partial rescue of ectopic shoot phenotype
402 to WT in these RNAi lines as an indicator of multiple shoot regulators regulated by
403 MEA and DME, as observed in their expression pattern (Figure 3A). Together, our
404 results suggest that MEA and DME act synergistically to regulate early shoot devel-
405 opment by repressing ectopic induction of shoot-promoting factors.

406 **Discussion**

407 The histone methyltransferase, MEDEA, and the DNA glycosylase, DEME-
408 TER, were initially identified as paternally imprinted genes expressed in the central
409 cell of the female gametophyte. Both act synergistically to restrict the over-
410 proliferation of the central cell in the absence of double fertilization (Moreno-Romero
411 *et al*., 2016). Ovules inheriting the strong mutant alleles of both *mea* and *dme* abort
412 seed development, making it impossible to recover homozygotes of either mutant.
413 The maternal lethality of the *mea* and *dme* alleles makes it challenging to examine
414 their roles beyond the gametophyte stage. However, recent studies have successful-
415 ly implemented various genetic strategies to obtain viable, single mu-
416 tant, *mea,* and *dme* homozygotes (Ravi *et al*., 2014; Pires *et al*., 2016; Kim *et al*.,
417 2021; Williams *et al*., 2022). These single mutants have helped demonstrate the role
418 of DME and MEA in various phases of sporophyte development, in addition to its pri-
419 or established role in the gametophytes. For instance, MEA is required for proper
420 embryonic patterning by regulating cell division via D-type cyclin 1.1 (CYCD1;1) (Si-
421 monini *et al.*, 2021). MEA also facilitates *P. syringae* infection in *Arabidopsis* by
422 downregulating RESISTANCE TO P. SYRINGAE2 (RPS2) (Roy *et al*., 2018). Like
423 MEA, DME also has a sporophytic role in controlling cell division rate in sporophytic
424 tissues like root hair and stomata, the maintenance of inflorescence meristem, and
425 *de novo* shoot regeneration (Kim *et al.*, 2021). DME, along with its somatic DNA de-
426 methylating counterparts, is also shown to regulate flowering time and inflorescence
427 meristem activity (Williams *et al.*, 2022; Kim *et al*., 2021). Like MEA, DME also re-
428 stricts pathogen infection by repressing transposable elements controlling disease-
429 related proteins in *Arabidopsis* (Schumann *et al*., 2019). In contrast to the docu-
430 mented single mutant phenotypes, *mea*-1$^{-/-}$;*dme*-2$^{-/-}$ plants show a unique presence
431 of twin shoots arising from seed with a single embryo suggesting the interplay of
432 both MEA and DME during seed to the seedling transition phase of sporophyte de-
433 velopment.

434 The rescue of *mea*-1$^{-/-}$;*dme*-2$^{-/-}$ haploid sporophytes using CenH3-
435 mediated genome elimination as a tool facilitated us to generate a population
436 of *mea*-1$^{-/-}$;*dme*-2$^{-/-}$ DH plants which in turn shed light on the synergistic role of MEA
437 and DME in suppressing the activation of ectopic shoot meristems during early spo-
438 rophyte development. Shoot developmental processes like regeneration and floral
439 transitions are known to be restricted by the repressive histone and DNA methylation

440 marks (Li *et al*., 2011; Sun *et al*., 2014). However, only a few studies have reported
441 the involvement of such epigenetic players during early sporophyte development
442 (Bouyer *et al*., 2011). Seed to seedling transition is controlled by FIE, a subunit of the
443 PRC2 complex (Bouyer *et al.*, 2011). Here we propose that, during sporophytic de-
444 velopment, MEA, another subunit of the PRC2 complex, and DME restrict the for-
445 mation of a single meristem at the apical pole by repressing shoot regulators. Con-
446 sistent with this hypothesis, we show that an array of shoot regulators gets upregu-
447 lated than WT levels in the *mea*-1$^{-/-}$;*dme*-2$^{-/-}$ mutants. A closer inspection of the epi-
448 genetic signatures (DNA methylation) near selected shoot regulators revealed per-
449 turbance from the normal levels (Figure 4). The loss of H3K27me3 and gain of DNA
450 methylation is likely sufficient to trigger a change in the chromatin state near these
451 genes, causing a de-repression of the genes controlling shoot development early in
452 the plant life cycle. Restoration of wild-type shoot apex by down-regulation of a se-
453 lect few shoot-promoting factors in *mea*-1$^{-/-}$;*dme*-2$^{-/-}$ mutant strengthen this mecha-
454 nistic framework. Likely, DME- and MEA-mediated epigenetic suppression of shoot-
455 promoting factors such STM, PLT5, and CUC2 restrict the coordinated interactions
456 between several fundamental cellular processes such as cell division and differentia-
457 tion at the apical pole of the plant's body axis during post-embryonic development.

458 In conclusion, we demonstrate an extended synergistic role for the gameto-
459 phytic epigenetic regulators DME and MEA during the seed-to-seedling transition of
460 sporophyte development. Our study provides the basic framework for understanding
461 the role of gametophytic lethals in sporophytic tissue development. Further studies
462 utilizing haploid induction for generating homozygous mutants may offer more in-
463 sights into plant growth development.

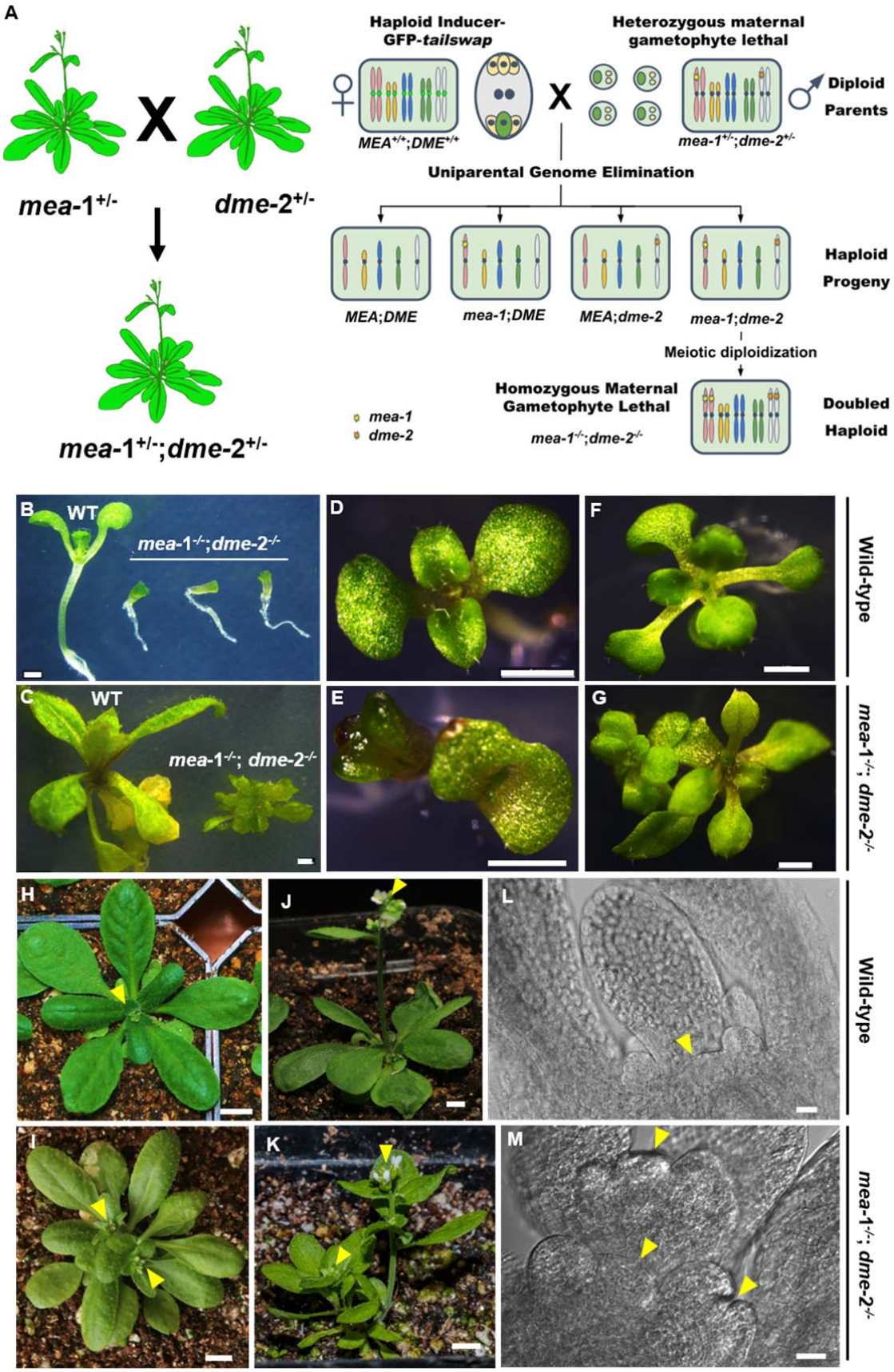
A
mea-1+/-
X
dme-2+/-
mea-1+/-;dme-2+/-
Haploid Inducer-GFP-tailswap
MEA+/+;DME+/+
X
Heterozygous maternal gametophyte lethal
mea-1+/-;dme-2+/-
Diploid Parents
Uniparental Genome Elimination
MEA;DME
mea-1;DME
MEA;dme-2
mea-1;dme-2
Haploid Progeny
Meiotic diploidization
Homozygous Maternal Gametophyte Lethal
mea-1-/-;dme-2-/-
Doubled Haploid
mea-1
dme-2
B WT
mea-1-/-;dme-2-/-
C WT
mea-1-/-; dme-2-/-
D
E
F
G
H
I
J
K
L
M
Wild-type
mea-1-/-; dme-2-/-
Wild-type
mea-1-/-; dme-2-/-

464

465 **Figure 1. Generation and phenotypic examination of *mea*-1 $^{-/-}$;*dme*-2 $^{-/-}$ plants**
466 **(A)** Schematic diagram illustrating rescue of *mea*-1$^{-/-}$;*dme*-2$^{-/-}$plants using CENH3-
467 mediated genome elimination. **(B,C)** Phenotype of *mea*-1$^{-/-}$;*dme*-2$^{-/-}$ seedlings as
468 compared to WT at 2- leaf (5 dpg) and 6-leaf (10 dpg) stage respectively. Repre-
469 sentative images of L*er* WT plants at **(D)** 2-leaf (5dpg), **(F)** 6-leaf (10 dpg), **(H)** inflo-
470 rescence emergence (21 dpg) and **(J)** flowering (28 dpg) stage as compared with
471 *mea*-1$^{-/-}$;*dme*-2$^{-/-}$ plants with ectopic shoot at **(E)** 2-leaf , **(G)** 6-leaf, **(I)** inflorescence
472 emergence and **(K)** flowering stages.
473 Longitudinal section of shoot apex of the 3-leaf stage (7 dpg) **(L)** L*er* WT and **(M)**
474 *mea*-1$^{-/-}$;*dme*-2$^{-/-}$ seedling. Yellow arrowhead is pointing at the shoot apex. Scale bar:
475 **(B-G)**= 1 mm; **(H-K)**= 5 mm; **(L-M)**= 20 µm. dpg: days post germination.

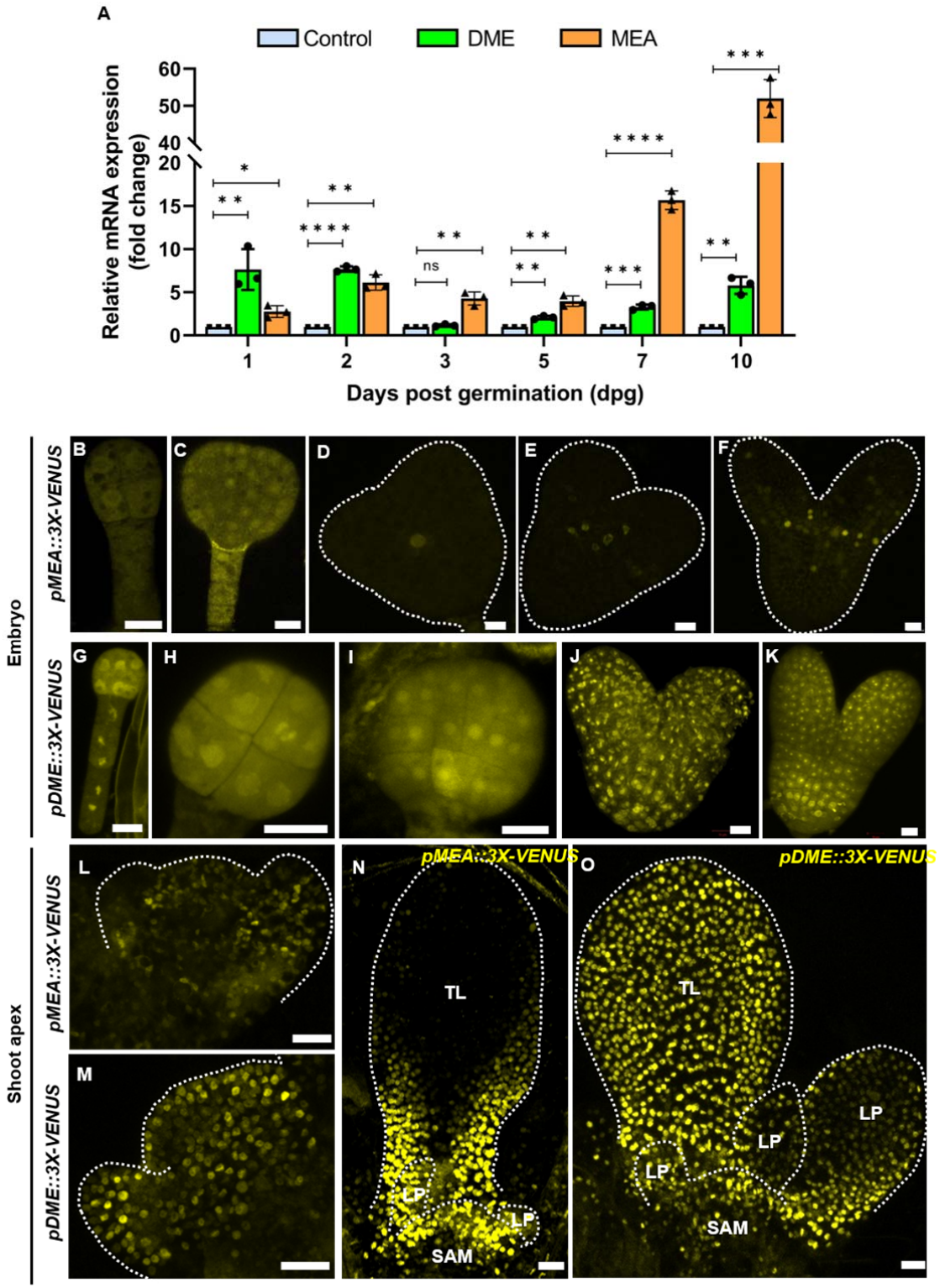

476

477 **Figure 2. Expression analysis of MEA and DME in sporophytic tissues (A)** Rela-
478 tive abundance of MEA and DME mRNA in developing seedlings. *DME* mRNA levels
479 are abundant in 1- and 2-dpg seedlings with sharp decrease in its level on 3- and 5-
480 dpg (1-dpg: 7.62±2.37, ***p*= 0.0016; 2-dpg: 7.69±0.30, *****p*= 0.000003; 3-dpg:

481 1.15±0.13, ^{ns}p= 0.11; 5-dpg: 2.06±0.20, **p= 0.003; 7-dpg: 3.28±0.29, ***p=0.00084;
482 10-dpg: 5.79±0.99, **p= 0.0033). *MEA* mRNA levels gradually increased as the
483 seedling transitioned from 1- to 10-dpg (1-dpg: 2.76±0.69, *p= 0.011; 2-dpg:
484 6.12±0.89, **p= 0.0023; 3-dpg: 4.27±0.76, **p= 0.0034; 5-dpg: 3.97±0.62, **p=
485 0.0033; 7-dpg: 15.66±1.08, ****p=0.0001; 10-dpg: 51.96±5.12, ***p= 0.00033). Sta-
486 tistical test: Multiple unpaired *t*-tests (Holm-Sidak method), with alpha = 0.05. Error
487 bar: SD.
488 **(B-O)** Representative images of embryos and shoot apices showing expression pat-
489 terns of **(B-F, L,N)** *pMEA*::3X- *VENUS* and **(G-K, M,O)** *pDME::*3X-*VENUS.*
490 *pMEA*::3X- *VENUS* expression (yellow) in developing embryo **(B)** octant, **(C)** globu-
491 lar, **(D)** early heart-shape, **(E,F)** heart-shape **(L)** SAM and in **(N)** shoot apex.
492 *pDME*::3X- *VENUS* expression (yellow) in developing embryo **(G)** octant, **(H)**
493 dermatogen **(I)** globular, **(J)** heart-shape **(K)** late heart-shape **(M)** SAM and **(O)** shoot
494 apex. SAM- shoot apical meristem, LP-leaf primordium, TL- true leaf. Scale bar: **(B-**
495 **K)**= 10 µm; **(L-O)**= 20 µm.

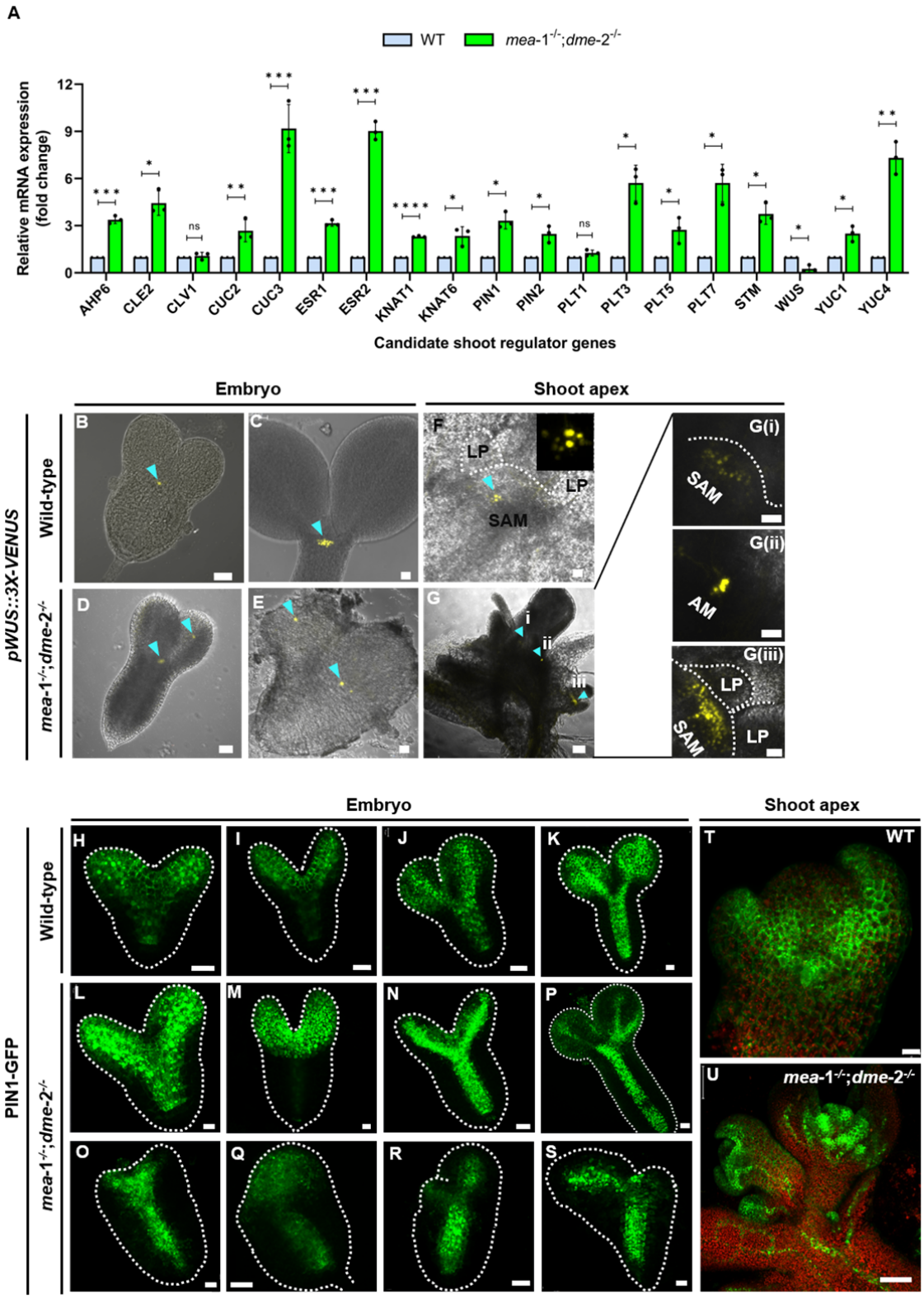
A
WT
mea-1-/-;dme-2-/-
Relative mRNA expression (fold change)
Candidate shoot regulator genes
AHP6
CLE2
CLV1
CUC2
CUC3
ESR1
ESR2
KNAT1
KNAT6
PIN1
PIN2
PLT1
PLT3
PLT5
PLT7
STM
WUS
YUC1
YUC4
Embryo
Shoot apex
pWUS::3X-VENUS
Wild-type
mea-1-/-;dme-2-/-
LP
SAM
AM
PIN1-GFP
WT

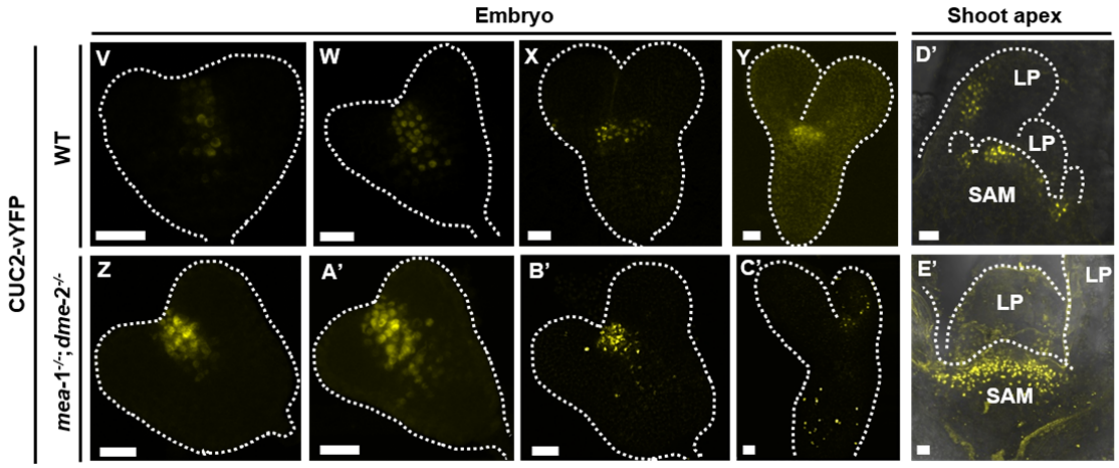

Figure 3. Deregulated expression pattern of shoot regulators in *mea*-1$^{-/-}$;*dme*-2$^{-/-}$ embryos and seedling (A) Relative abundance of shoot regulators in 2-3 dpg old *mea*-1$^{-/-}$;*dme*-2$^{-/-}$ seedlings compared with WT (fold change). *AHP6*: 3.78±0.24, ***p=0.0011; *CLE2*: 4.43±0.78, *p=0.019; *CLV1*: 1.08±0.22, ^{ns}p=0.571; *CUC2*: 2.52±0.87, **p=0.014; *CUC3*: 9.18±1.54, ***p=0.01; *ESR1*: 3.15±0.19, ***p=0.0006; *ESR2*: 9.02±0.58, ***p=0.0003; *KNAT1*: 2.30±0.19, ****p=0.00002; *KNAT6*: 2.35±0.59, *p=0.016; *PIN1*: 3.31±0.51, *p=0.019; *PIN2*: 2.47±0.53, *p=0.049; *PLT1*: 1.26±0.19, ^{ns}p=0.13; *PLT3*: 5.71±1.14, *p=0.021; *PLT5*: 2.73±0.82, *p=0.021; *PLT7*: 5.71±1.19, *p=0.021; *STM*: 3.74±0.65, *p=0.021; *WUS*: 0.26±0.22, *p=0.03; *YUC1*: 2.49±0.49, *p=0.042; *YUC4*: 7.32±1.03, **p=0.0067. N=3, statistical test: Multiple unpaired *t*-tests (Holm-Sidak method), with alpha = 0.05. Error bar: SD.

(B-E') Representative images of embryos and shoot apices showing expression pattern of **(B-H3)** *pWUS*::3X-*VENUS,* **(H-U)** PIN1-GFP and **(V-E')** CUC2-vYFP shoot regulators.

pWUS::3X-*VENUS* expression (yellow) in organizing center of embryos of **(B-C)** wild-type and **(D-E)** *mea*-1$^{-/-}$;*dme*-2$^{-/-}$ (n= 26/78) showing ectopic organizing center in cotyledon (marked with yellow arrowhead). *pWUS*::3X-VENUS is marking center of shoot meristem in **(F)** wild-type, inset is showing organizing center in SAM and **(G to G(iii))** *mea*-1$^{-/-}$;*dme*-2$^{-/-}$,along with **(G(i))** primary shoot meristem **(G(ii))** axillary meristem and **(G(iii))** ectopic shoot meristem, marked with blue arrowhead (n=21/48). The meristem dome (SAM) and leaf primordia (LP) are labeled and indicated with a white dashed line. The scale bar represents 20 µm in **(B-F)** and **(G(i) to G(iii))**, and 100 µm in **(G)**.

521 **(H-U)** PIN1-GFP (green) expression in embryos of **(H-K)** wild-type and **(L-S)** *mea*-1 -
522 /-;*dme*-2 -/- showing ectopic PIN1 expression. Dashed lines outline the embryo shape.
523 PIN1-GFP expression in shoot meristem of **(T)** wild-type **(U)** *mea*-1$^{-/-}$;*dme*-2$^{-/-}$ seed-
524 ling showed PIN1 expression in ectopic shoot along with primary shoot (n=29/55)
525 along with red as autofluorescence. The scale bar represents 20 µm in **(H-S)** and100
526 µm in **(T-U)**.
527 **(V-E')** CUC2-vYFP (yellow) expression in embryos of **(V-Y)** wild-type and **(Z- C')**
528 *mea*-1$^{-/-}$;*dme*-2$^{-/-}$ showing ectopic expression at SAM and developing cotyledons (n=
529 31/77). CUC2-vYFP expression in shoot apex of **(D')** wild-type and **(E')** *mea*-1$^{-/-}$
530 ;*dme*-2$^{-/-}$ showing ectopic expression in SAM apart from leaf primordia (n= 15/77).
531 The scale bar represents 20 µm. SAM- shoot apical meristem, AM- axillary meri-
532 stem, LP-leaf primordium.
533

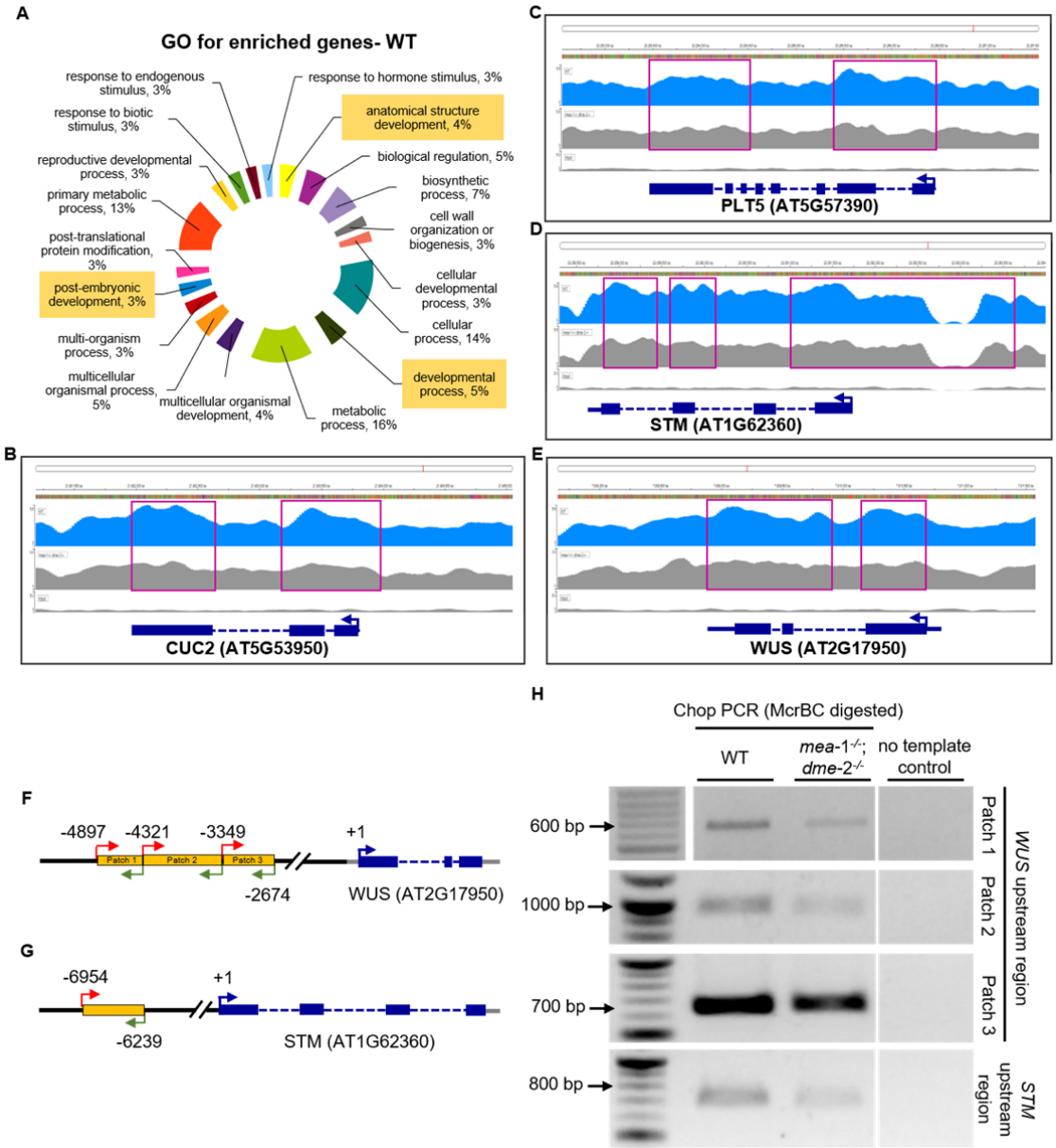

Figure 4. Validation of targets of MEA and DME (A) Gene ontology (GO) of enriched genes in ChIP using αH3K27me3. **(B-E)** Graphical representation of ChIP-seq using αH3K27me3 for **(B)** *STM*, **(C)** *CUC2* **(D)** *PLT5* and **(E)** *WUS* gene and their upstream region. Pink boxes denote prominent enrichment in WT ChIP DNA as compared to *mea*-1$^{-/-}$;*dme*-2$^{-/-}$ ChIP DNA. Input DNA is WT DNA without αH3K27me3 treatment. **(F-G)** Cartoon representation of *WUS* and *STM* upstream regions showing putative methylated regions (yellow box) and corresponding forward (red) and reverse (green) oligonucleotides used for Chop PCR. **(H)** Lower amplification in McrBC-chop PCR of hypermethylated regions of *WUS*, and *STM* upstream regions

544 in *mea*-1$^{-/-}$;*dme*-2$^{-/-}$ as compared to hypomethylated WT. Black line: upstream region,
545 gray line: UTR, blue box: exon, blue dotted line: intron.
546

547

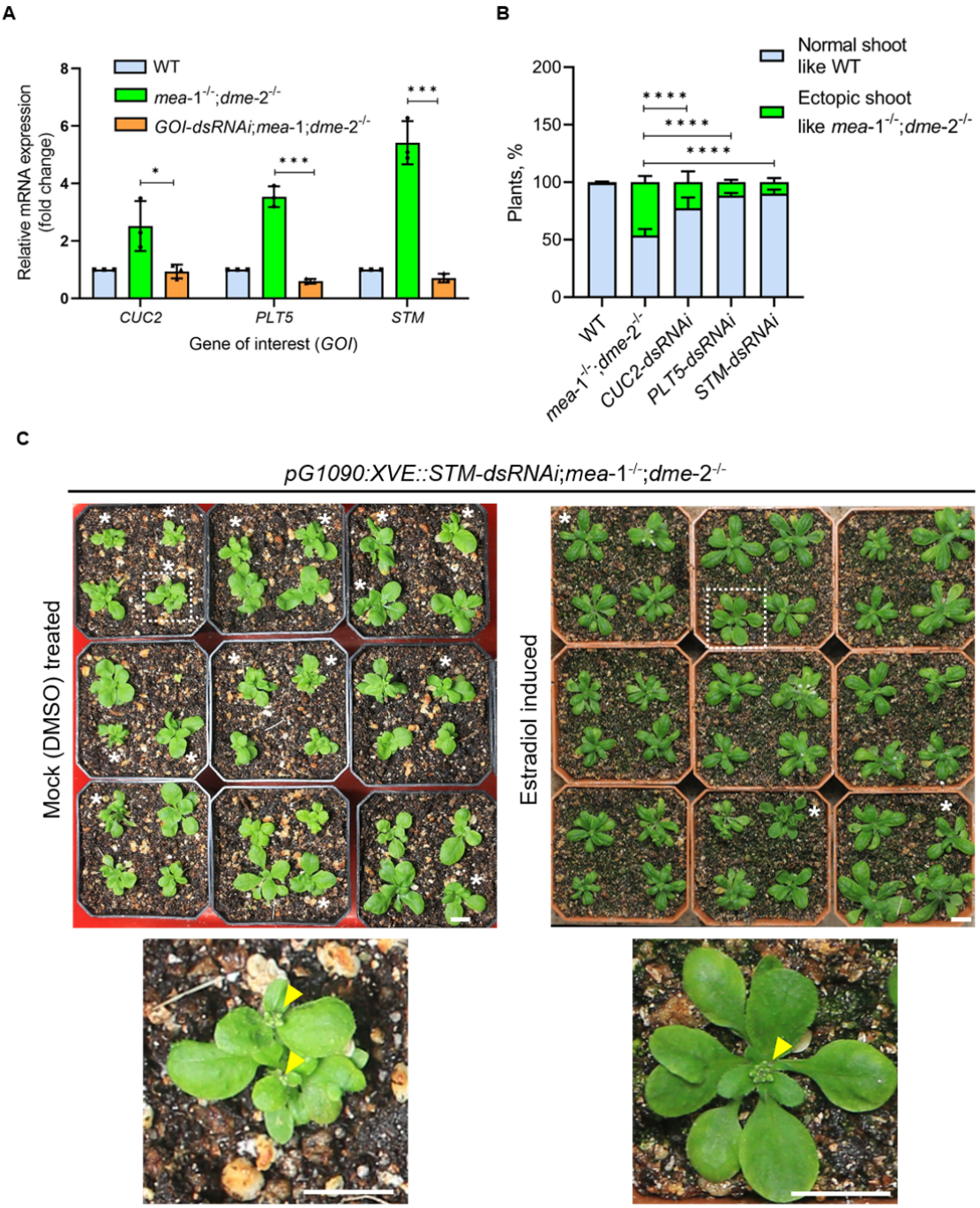

548

549 **Figure 5. RNAi mediated downregulation of select target genes. (A)** Relative
550 abundance of *CUC2*, *PLT5*, and *STM* transcripts in respective RNAi lines. *CUC2*:
551 WT- 1±0, *mea*-1$^{-/-}$;*dme*-2$^{-/-}$- 2.52±0.87, *CUC2*-dsRNAi;*mea*-1$^{-/-}$;*dme*-2$^{-/-}$- 0.94±0.24,
552 **p*=0.038; *PLT5*: WT- 1±0, *mea*-1$^{-/-}$;*dme*-2$^{-/-}$- 3.54±0.36, *PLT5*-dsRNAi;*mea*-1$^{-/-}$;*dme*-
553 2$^{-/-}$- 0.60±0.08, ****p*=0.00048; *STM*: WT- 1±0, *mea*-1$^{-/-}$;*dme*-2 $^{-/-}$- 5.42±0.75, *STM*-

554 dsRNAi;*mea*-1$^{-/-}$;*dme*-2$^{-/-}$- 0.71±0.15, ***p=0.0008. Statistical test: Multiple unpaired
555 *t*-tests (Holm-Sidak method), with alpha = 0.05. Error bar: SD.
556 **(B)** Quantification of shoot number in *CUC2*-, *PLT5*- and *STM*-RNAi lines as com-
557 pared to WT and *mea*-1$^{-/-}$;*dme*-2$^{-/-}$. WT: n= 161 (Normal shoot= 161, ectopic shoot=
558 0); *mea*-1$^{-/-}$;*dme*-2$^{-/-}$: n= 139 (Normal shoot= 71, ectopic shoot= 68); *CUC2*-
559 dsRNAi;*mea*-1$^{-/-}$;*dme*-2$^{-/-}$: n= 134 (Normal shoot= 102, ectopic shoot= 32, ****p<
560 0.0001); *PLT5*-dsRNAi;*mea*-1$^{-/-}$;*dme*-2$^{-/-}$: n= 231 (Normal shoot= 203, ectopic shoot=
561 32, ****p< 0.0001); *STM*-dsRNAi;*mea*-1$^{-/-}$;*dme*-2$^{-/-}$: n= 98 (Normal shoot= 89, ectopic
562 shoot= 9, ****p< 0.0001). Statistical analysis: two-way ANOVA (Sidak method), with
563 alpha = 0.05. Error bar: SEM.
564 **(C)** Rescue of ectopic shoot in estradiol-induced *STM*-dsRNAi;*mea*-1$^{-/-}$;*dme*-2$^{-/-}$
565 plants. Asterix(*) marks plants with ectopic shoots. White dotted box corresponds to
566 the zoomed plants shown in the below panel. Yellow arrowhead points to the shoot
567 apex. Scale bar: 1cm.

568

Materials and Methods

Plant materials and growth conditions

Arabidopsis thaliana seeds were surface sterilized by fumigation with Chlorine (Cl_2) gas (Lindsey III *et al*., 2017). Fumigated seeds were then plated onto Murashige and Skoog (MS) growth medium with 0.8% agar and cold stratified at 4℃ in dark for four days. After cold stratification, the plates were transferred to the growth chamber for germination. Seedlings and plants in pots were grown under white fluorescent lights (7000 lux at 20 cm) at 22 °C with a 16 h light/8 h dark cycle at 75% RH in a controlled growth cabinet (Percival Inc.). Heterozygous *MEA*/*mea*-1 (Grossniklaus *et al*., 1998) and *DME*/*dme*-2 (Choi *et al*., 2002) mutants were previously described. Following heterozygous seeds were obtained from Arabidopsis Biological Resource Center: *MEA*/*mea*-6 (CS6996), *MEA*/*mea*-7 (CS6997), *DME*/*dme*-6 (GK-252E03), and *DME*/*dme*-7 (SALK107538).

Generation of maternal gametophytic lethal homozygotes

To generate *dme*-2 (AT5G04560) and *mea*-1 (AT1G02580) homozygous mutants, heterozygous *DME*/*dme*-2 and *MEA*/*mea*-1 plants were crossed as the male to haploid inducer GFP-*tailswap* plants as female (Ravi *et al*., 2014). The resultant F1 seeds were collected and germinated on Murashige and Skoog agar plates and later transferred to soil for further growth. Haploids were identified phenotypically and cytologically as described earlier (Ravi and Bondada, 2016). All the haploids were PCR genotyped to identify the *DME* WT allele using MR146 and MR147 oligo combinations amplifying a 791 bp fragment. Similarly, the *dme*-2 mutant haploids were identified using MR147 and a left border-specific oligo MR148 producing 381 bp fragment. For *MEDEA*, the WT allele was identified using oligonucleotides combinations MR8 and MR319 (722 bp), and the *mea*-1 allele using MR8 and a left border-specific oligo MR10 (312 bp). The DNA sequences for all oligos used in this study is given in Supplementary Table 4. The mutant haploids were screened for spontaneous mitotic/meiotic doubling events for obtaining doubled haploid seeds which gives rise to homozygous mutant diploid sporophytes. For generating homozygous *mea*-1;*dme*-2 double mutant in L*er* ecotype, *mea*-1 homozygous plants serving as female parent were crossed with *dme*-2 heterozygous plants as male parent. The resulting progeny PCR genotyped for both the *mea*-1 and *dme*-2 alleles, and the plants heterozygous

602 plant both *mea*-1 and *dme*-2 alleles were identified and used as male parent in a
603 cross with GFP-*tailswap* as female. *mea*-1;*dme*-2 haploid plants were identified us-
604 ing PCR-based genotyping. Spontaneous double haploid seeds from *mea*-1;*dme*-2
605 plants were collected to generate *mea*-1;*dme*-2 doubled haploid (diploid) sporo-
606 phytes used in this study.
607
608 **Quantitative Real Time-PCR**
609 For expression analysis of *DME* and *MEA* mRNA, we harvested shoot apices from 1,
610 3, 5, 7, and 10 dpg old WT seedlings and stored at -80℃ for further use. Shoot api-
611 ces from *mea*-1$^{-/-}$;*dme*-2$^{-/-}$ seedlings were used as control. Similarly, for expression
612 analysis of selective shoot regulators and somatic epigenetic factors, we harvested
613 shoot apices from 2 to 3-day-old WT and *mea*-1$^{-/-}$;*dme*-2$^{-/-}$ seedlings. Total RNA was
614 isolated using TRIzol™ reagent as per the manufacturer's instructions. The extracted
615 RNA was treated with NEB(New England Biolabs) DNase I (RNase free) (M0303)
616 according to NEB guidelines to remove the genomic DNA contamination. One mi-
617 crogram of total RNA was used for complementary DNA (cDNA) synthesis by
618 PrimeScript first strand cDNA synthesis kit (TAKARA-Bio, Cat# 6110) using an oli-
619 go(dT) and random hexamer as oligonucleotides. qPCRs were performed on Mas-
620 tercycler BIORAD CFX96™ using the oligonucleotides mentioned in Supplementary
621 Table T4. *ACTIN2* (*ACT2*) served as a reference gene control. The reactions were
622 carried out using TB Green® Premix Ex Taq™ II (TAKARA-Bio, Cat no. RR82WR)
623 and incubated at 95 °C for 2 minutes, followed by 40 cycles of 95 °C for 15 s and 60
624 °C for 30 s. PCR specificity was checked by melting curve analysis. *ACT2* was used
625 for the normalization for all the reactions. At least three independent biological sam-
626 ples were analyzed for each time point mentioned above, and qPCR reactions were
627 set up with three technical replicates for each biological replica. mRNA abundance of
628 target genes was analyzed using the normalized $2^{-\Delta\Delta Ct}$ (cycle threshold) method
629 (Livak and Schmittgen, 2001).
630
631 **ChIP followed by Next-Generation Sequencing**
632 To identify the targets of MEA protein and differentiate histone methylation, we per-
633 formed chromatin immunoprecipitation (ChIP) followed by next-generation sequenc-
634 ing as described previously (Salvi *et al*., 2020; Yamaguchi *et al*., 2014) on two inde-
635 pendent biological replicates. 500 mg of micro dissected shoot apices, devoid of cot-

636 yledons and hypocotyl, from 2 to 3-day-old WT and *mea*-1$^{-/-}$;*dme*-2$^{-/-}$ seedlings were
637 used for each sample. The samples were fixed in 1.8% formaldehyde in 1X PBS and
638 vacuum infiltrated for 15 mins at room temperature to cross-link the tissue. After fixa-
639 tion, formaldehyde solution was removed and replaced by ice-cold 0.125 M glycine
640 solution (in 1X PBS) followed by vacuum infiltration for 5 mins to quench the reac-
641 tion. The glycine solution was filtered away and samples were washed twice with ice-
642 cold 1X PBS. Samples were blotted on Kim wipe paper to remove excess 1X PBS.
643 Samples were frozen and powdered in liquid nitrogen. The powdered samples were
644 resuspended in nuclei extraction buffer (50 mM Tris-HCl pH 7.5, 150 mM NaCl, 1%
645 Triton X-100, 0.1% sodium deoxycholate, 2.5 mM EDTA, 10% glycerol, freshly sup-
646 plemented with cOmplete™, EDTA-free protease inhibitor cocktail (Cat#
647 04693132001) and 1 mM PMSF (Sigma). After brief incubation of 15 minutes, sam-
648 ple solutions were filtered using Falcon® 40 µm cell strainer (Cat# 352340). Filtrate
649 was centrifuged at 4°C to pellet the nuclei. The pellet was resuspended in an ice-
650 cold nuclei lysis buffer (50 mM Tris-HCl, pH 8; 5 mM EDTA, pH 8; 0.5% SDS). The
651 solution was sonicated for 8 cycles of 10 seconds with 20 seconds gap at 39% am-
652 plitude (Branson Sonifier, Marshall Scientific). 1.1% triton was added to the sonicat-
653 ed sample and centrifuged to isolate the supernatant. Preclearing of the sample was
654 done by adding 20 µl of Dynabeads™ Protein G (Invitrogen, Cat# 10003D) and in-
655 cubated at 4 ℃ for 2h. An aliquot of the sample was stored as Input for the experi-
656 ment. The sample was incubated with mouse monoclonal antibody to H3K27me3
657 (ab6002; Abcam) overnight at 4℃, and dynabeads protein was added to immuno-
658 precipitate the DNA fragment for 5 hr at 4℃. Sequential washes were performed in
659 the beads using cold low salt wash buffer (150 mM NaCl, 0.2% SDS, 0.5% Triton X-
660 100, 2 mM EDTA pH 8, 20 mM Tris-HCl pH 8), cold high salt wash buffer (500 mM
661 NaCl, 0.2% SDS, 0.5% Triton X-100, 2 mM EDTA pH 8, 20 mM Tris-HCl pH 8), cold
662 250mM LiCl wash buffer (0.25 M LiCl, 0.5% NP-40, 0.5% sodium deoxycholate, 1
663 mM EDTA pH 8, 10 mM Tris-HCl pH 8) and 0.5X TE. All washes were done twice.
664 Magnetic beads were collected and resuspended in TES (25 mM Tris-HCl pH 8, 5
665 mM EDTA pH 8, 0.5% SDS). 5 M NaCl was added to the sample and input control to
666 reverse the cross-links overnight at 65℃. DNA fragments were purified using a PCR
667 purification kit (Cat #28106, Qiagen). Library constructions were performed, and val-

668 idated using Qubit and Agilent TapeStation, followed by 150bp paired-end sequenc-
669 ing on Illumina NovaSeq 6000 by miBiome Therapeutics LLP, Mumbai, India.
670 The trimmed reads were aligned to reference genome TAIR10, using BWA 0.7.17-
671 r1188 (Li, 2013). The quality check of the alignments was done using Qualimap
672 2.2.2-dev (Okonechnikov *et al*., 2015). Duplicated reads, reads with low mapping
673 quality, and mitochondrial and plastid reads were identified and removed with
674 Samtools version 1.2 (Li *et al*., 2009). Enriched intervals between the IP sample and
675 its relative Input were identified by MACS2 (version 2.0.10) program (Zhang *et al*.,
676 2008) with the default setting. The big-Wig files were generated from the BAM files
677 using Deeptools 3.5.1 (Ramirez *et al*., 2016). The coverage is calculated as the
678 number of reads per bin and normalized to 1 x sequencing depth (reads per genome
679 coverage, RPGC). The resulting bigWig files were visualized in Integrated Genome
680 Viewer (https://igv.org/app/)(Robinson *et al*., 2011) to observe the protein binding on
681 the chromatin. Peak annotation and GO and KEGG analysis for the target regions
682 were done using ChIPseeker 1.32.1 (Yu *et al*., 2015) and ClusterProfiler 4.4.4 (Yu *et*
683 *al*., 2012).
684
685 **Chop-PCR assay**
686 Genomic DNA from 2 to 3 dpg old WT and *mea*-1$^{-/-}$;*dme*-2$^{-/-}$ seedlings was isolated
687 using the standard CTAB method. One microgram of DNA was digested with meth-
688 ylation-sensitive restriction enzyme McrBC (NEB, Cat# M0272) at a concentration of
689 10 units/µg of DNA template in a 30 µl reaction mix, as per manufacturer's instruc-
690 tion, for at least 6 h. After heat inactivation, 4 µl of the digested DNA was used as a
691 template in a 20 µl reaction volume for PCR for 25 cycles.
692
693 **Microscopy and imaging**
694 Bright-field images of seedlings were captured using Leica M205FA stereo micro-
695 scope. Confocal laser scanning microscopic images were acquired using Zeiss LSM
696 880 and Leica TCS SP5 II confocal laser-scanning microscope. The confocal imag-
697 ing was carried out on dissected embryos and 3 to 5 dpg old seedlings using Argon
698 laser source at 40% power. The excitation wavelengths were as follows: 488 nm- for
699 GFP and 514 nm- for YFP. Auto-fluorescence was captured at the wavelength of
700 633 nm. Images were captured with 40x (oil) or 63x (oil) objectives with 550-750
701 master gain, 100-200 range pinhole, and frame size of 1,024 by 1,024 pixels. Master

gain and the pinhole adjustment varied with samples. The line averaging was adjusted to four and the digital zoom to 0.6. Z-stack images were taken in 5 µm or 1 µm intervals. The whole plant images are captured using a Canon 70D SLR camera. The images are edited in Adobe Photoshop CS4.

Plasmid construction, molecular cloning, and plant transformation

For cloning the gene and its regulatory sequences, the sequence of interest was PCR amplified from total genomic DNA isolated by CTAB method. For cDNA cloning, total RNA was isolated using TRIzol™ reagent as per the manufacturer's instructions. One microgram of DNase-free RNA was used for cDNA synthesis by PrimeScript 1st strand cDNA synthesis kit using an oligo(dT) and random hexamer as oligonucleotides . Polymerase chain reaction (PCR) was carried out using PrimeSTAR® GXL DNA Polymerase (TAKARA-Bio, Cat# R050). The PCR conditions were specific to each sequence and amplified using 10 µM sequence-specific paired oligonucleotides (see Supplementary Table T4) using Applied Biosystems™ ProFlex™ 3 x 32-well PCR System. All entry clones were propagated in DH5α strain of *E.coli* using a single Gateway cloning system. To knock down the expression of *STM*, 272 bp exon sequence was amplified from *cDNA* using region-specific oligonucleotides and cloned in the p2R3E-As-OScT vector (sense) and p221Z-S-Intr vector (antisense) using *Bam*HI and *Xho*I restriction digestion and ligation. All entry clones were propagated in the DH5α strain of E.coli using a single gateway cloning system. The sense and antisense for STM were cloned under *pG1090* inducible promoter (Zuo *et al*., 2000) and subsequently in *pCAMBIA-based R4R3* destination vector. Similarly, the *PLT5* (299 bp) and *CUC2* (Varapparambath *et al*., 2022) knockdown constructs were cloned under *pG1090* inducible promoter to silence the transcript level of *PLT5* and *CUC2*, respectively. To generate *pDME*::*3X-VENUS*:*3AT*, 5000bp upstream regulatory sequence of *DME* is tagged with *3X-VENUS* and *3AT* terminator. Similarly, 5142bp of *MEA* promoter was tagged with *3X-VENUS* to generate *pMEA*::*3X-VENUS*:*3AT*. Translation fusion lines of DME (*pDME*::*gDME*:*vYFP*) and MEA (*pMEA*::*gMEA*:*vYFP*) were generated using three fragments multisite recombination gateway cloning system where the above-mentioned upstream regulatory sequences of *DME* and *MEA* were cloned to drive *DME* (8303 bp) and *MEA* (4199 bp) genomic sequences fused with *vYFP*.

736 **Estradiol treatment for inducible gene knock-down**

737 Inducible RNAi for *STM*, *PLT5*, and *CUC2* genes was carried out, as mentioned ear-
738 lier (Varapparambath *et al*., 2022). MS agar medium supplemented with 5μM β-
739 estradiol was used to induce conditional gene silencing using *pG1090*:*XVE* artificial
740 promoter throughout seed germination. Estradiol-treated and mock (DMSO) treated
741 seedlings were scored for ectopic shoot emergence at 15 dpg.

742

743 **Statistical analysis**

744 The details of the statistical analysis followed in this study are described in the re-
745 spective figure legends (number of samples (n), mean± S.E.M). The statistical signif-
746 icance levels were defined as $*p < 0.05$, $**p < 0.01$, $***p < 0.001$, $****p < 0.0001$. For
747 mRNA quantitative analysis, statistical significance was determined using the Multi-
748 ple unpaired *t*-tests (Holm-Sidak method), with alpha = 0.05. For RNAi phenotype
749 quantitative analysis, statistical significance was determined using two-way ANOVA
750 (Sidak method), with alpha = 0.05. All the statistical tests and analyses were per-
751 formed using GraphPad PRISM (v9.5.1) statistical software.

752

753 **Data Availability**

754 The ChIP-sequencing data generated and analyzed during the current study are
755 available from NCBI under the bio project accession PRJNA972183 consisting of six
756 SRA accession identifiers: SRR24547737**,** SRR24547736**,** SRR24547733,
757 SRR24547734, SRR24547735, and SRR24547732. All other source data are in-
758 cluded in the article as Supplementary Table T3.

759

760 **Acknowledgments**

761 M.P.R. thanks to the IISER Thiruvananthapuram for providing a Ph.D. research fel-
762 lowship. S.S. is a recipient of the Department of Science and Technology (DST) -
763 INSPIRE scholarship for higher education (SHE). R.B. is the recipient of a Junior and
764 Senior Research Fellowship (J.R.F. and S.R.F.) for a Ph.D. funded by the University
765 Grants Commission (U.G.C.), Govt. of India. A.P.S. thanks to the Council of Scien-
766 tific and Industrial Research (CSIR) for the Ph.D. fellowship. K.P. acknowledges
767 grants from the Department of Biotechnology (D.B.T.), Government of India
768 (BT/PR41931/BRB/10/1964/2021), the Science and Engineering Research Board-
769 Scientific and Useful Profound Research Advancement (SERB-SUPRA), Govern-

ment of India (S.P.R./2021/000109). R.M. acknowledges financial support from Ramalingaswami's re-entry fellowship awarded by the Department of Biotechnology (D.B.T., Govt. of India) and the Dupont Young Professor grant, Dupont U.S.A. We thank the Indian Institute of Science Education and Research (IISER)- Thiruvananthapuram for intramural financial and infrastructural support.

Author contributions

R.M. conceptualized, designed, and supervised the study. M.P.R. contributed to certain aspects of the study design and carried out most of the experiments. S.S. generated and performed the phenotypic assessment of RNAi lines along M.P.R. R.B. helped generate double mutant lines. A.P.S. performed cloning experiments for producing reporter lines. K.P. designed, supervised, and critically analyzed the study. M.P.R., K.P., and R.M. wrote the manuscript. R.M. and K.P. acquired funds for the study. All the authors read and approved the draft.

Declaration of interests

The authors declare no competing interests.

References

1. Aichinger, E., Villar, C.B.R., Di Mambro, R., Sabatini, S., and Köhler, C. (2011). The CHD3 Chromatin Remodeler PICKLE and Polycomb Group Proteins Antagonistically Regulate Meristem Activity in the *Arabidopsis* Root. Plant Cell 23: 1047–1060.

2. Aida, M., Ishida, T., and Tasaka, M. (1999). Shoot apical meristem and cotyledon formation during *Arabidopsis* embryogenesis: Interaction among the *CUP-SHAPED COTYLEDON* and *SHOOT MERISTEMLESS* genes. Development 126: 1563–1570.

3. Aida, M., Vernoux, T., Furutani, M., Traas, J., and Tasaka, M. (2002). Roles of PIN-FORMED1 and MONOPTEROS in pattern formation of the apical region of the *Arabidopsis* embryo. Development 129: 3965–3974.
4. Borg, M., Jacob, Y., Susaki, D. *et al.* (2020).Targeted reprogramming of H3K27me3 resets epigenetic memory in plant paternal chromatin. Nat Cell Biol 22: 621–629.

5. Bouyer, D., Kramdi, A., Kassam, M., Heese, M., Schnittger, A., Roudier, F., and Colot, V. (2017). DNA methylation dynamics during early plant life. Genome Biol. 18: 1–12.

6. Bouyer, D., Roudier, F., Heese, M., Andersen, E.D., Gey, D., Nowack, M.K., Goodrich, J., Renou, J.P., Grini, P.E., Colot, V., and Schnittger, A. (2011). Polycomb repressive complex 2 controls the embryo-to-seedling phase transition. PLoS Genet. 7.

7. Burian, A., Raczyńska-Szajgin, M., Borowska-Wykręt, D., Piatek, A., Aida, M., and Kwiatkowska, D. (2015). The *CUP-SHAPED COTYLEDON2* and *3* genes have a post-meristematic effect on *Arabidopsis thaliana* phyllotaxis. Ann. Bot. 115: 807–820.

8. Chaudhury, A.M., Ming, L., Miller, C., Craig, S., Dennis, E.S., and Peacock, W.J. (1997). Fertilization-independent seed development in *Arabidopsis thaliana*. Proc. Natl. Acad. Sci. U. S. A. 94: 4223–4228.

9. Chen, D., Molitor, A., Liu, C., and Shen, W.H. (2010). The *Arabidopsis* PRC1-like ring-finger proteins are necessary for repression of embryonic traits during vegetative growth. Cell Res. 20: 1332–1344.

10. Choi, Y., Gehring, M., Johnson, L., Hannon, M., Harada, J.J., Goldberg, R.B., Jacobsen, S.E., and Fischer, R.L. (2002). DEMETER, a DNA glycosylase domain protein, is required for endosperm gene imprinting and seed viability in *Arabidopsis*. Cell 110: 33–42.

11. Cui, X. *et al*. (2016). REF6 recognizes a specific DNA sequence to demethylate H3K27me3 and regulate organ boundary formation in *Arabidopsis*. Nat. Genet. 48: 694–699.

12. Daimon, Y., Takabe, K., and Tasaka, M. (2003). *The CUP-SHAPED COTYLEDON* Genes Promote Adventitious Shoot Formation on Calli. Plant Cell Physiol. 44: 113–121.

13. Dasgupta, P. and Chaudhuri, S. (2019). Analysis of DNA Methylation Profile in Plants by Chop-PCR. In Plant Innate Immunity, W. Gassmann, ed, Methods in Molecular Biology. (Springer New York: New York, NY), pp. 79–90.

14. De Lucia, F., Crevillen, P., Jones, A.M.E., Greb, T., and Dean, C. (2008). A PHD-polycomb repressive complex 2 triggers the epigenetic silencing of FLC during vernalization. Proc. Natl. Acad. Sci. U. S. A. 105: 16831–16836.

15. Du, J., Johnson, L.M., Jacobsen, S.E., and Patel, D.J. (2015). DNA methylation pathways and their crosstalk with histone methylation. Nat. Rev. Mol. Cell Biol. 16: 519–532.

16. Feng, J., Liu, T., Qin, B., Zhang, Y., and Liu, X.S. (2012). Identifying ChIP-seq enrichment using MACS. Nat. Protoc. 7: 1728–1740.

17. Figueiredo, D.D., Batista, R.A., Roszak, P.J., and Köhler, C. (2015). Auxin production couples endosperm development to fertilization. Nat. Plants 1.

18. Gehring, M., Bubb, K.L., and Henikoff, S. (2009). Extensive Demethylation of Repetitive Elements During Seed Development Underlies Gene Imprinting. Science 324: 1447–1451.

19. Gehring, M., Huh, J.H., Hsieh, T.F., Penterman, J., Choi, Y., Harada, J.J., Goldberg, R.B., and Fischer, R.L. (2006). DEMETER DNA glycosylase establishes MEDEA polycomb gene self-imprinting by allele-specific demethylation. Cell 124: 495–506.

20. Gong, Z., Morales-Ruiz, T., Ariza, R.R., Roldán-Arjona, T., David, L., and Zhu, J.K. (2002). ROS1, a repressor of transcriptional gene silencing in *Arabidopsis*, encodes a DNA glycosylase/lyase. Cell 111: 803–814.

21. Grossniklaus, U., Vielle-Calzada, J.P., Hoeppner, M.A., and Gagliano, W.B. (1998). Maternal control of embryogenesis by *MEDEA*, a Polycomb group gene in *Arabidopsis*. Science 280: 446–450.

22. Guitton, A.-E., Page, D.R., Chambrier, P., Lionnet, C., Faure, J.-E., Grossniklaus, U., and Berger, F. (2004). Identification of new members of Fertilization Independent Seed Polycomb Group pathway involved in the control of seed development in *Arabidopsis thaliana*. Development 131: 2971–81.

23. Gutzat, R. *et al*. (2020). *Arabidopsis* shoot stem cells display dynamic transcription and DNA methylation patterns. EMBO J. 39.

24. Heisler, M.G., Ohno, C., Das, P., Sieber, P., Reddy, G.V., Long, J.A., and Meyerowitz, E.M. (2005). Patterns of auxin transport and gene expression during primordium development revealed by live imaging of the *Arabidopsis* inflorescence meristem. Curr. Biol. 15: 1899–1911.

25. Higo, A. *et al*. (2020). DNA methylation is reconfigured at the onset of reproduction in rice shoot apical meristem. Nat. Commun. 11: 1–12.

26. Hofhuis, H., Laskowski, M., Du, Y., Prasad, K., Grigg, S., Pinon, V., and Scheres, B. (2013). Phyllotaxis and rhizotaxis in *Arabidopsis* are modified by three plethora transcription factors. Curr. Biol. 23: 956–962.

27. Ibarra, C.A. *et al*. (2012). Active DNA Demethylation in Plant Companion Cells Reinforces Transposon Methylation in Gametes. Science 337: 1360–1364.

28. Iwasaki M and Paszkowski J (2014) Epigenetic memory in plants. EMBO J. 33: 1987-1998.
    a.

29. Kareem, A., Durgaprasad, K., Sugimoto, K., Du, Y., Pulianmackal, A.J., Trivedi, Z.B., Abhayadev, P.V., Pinon, V., Meyerowitz, E.M., Scheres, B., and Prasad, K. (2015). *PLETHORA* genes control regeneration by a two-step mechanism. Curr. Biol. 25: 1017–1030.

30. Khouider, S., Borges, F., LeBlanc, C., Ungru, A., Schnittger, A., Martienssen, R., Colot, V., and Bouyer, D. (2021). Male fertility in *Arabidopsis* requires active DNA demethylation of genes that control pollen tube function. Nat. Commun. 12: 1–10.

31. Kim, M., Ohr, H., Lee, J.W., Hyun, Y., Fischer, R.L., and Choi, Y. (2008). Temporal and spatial downregulation of *Arabidopsis* MET1 activity results in global DNA hypomethylation and developmental defects. Mol. Cells 26: 611–615.

32. Kim, S., Park, J.S., Lee, J., Lee, K.K., Park, O.S., Choi, H.S., Seo, P.J., Cho, H.T., Frost, J.M., Fischer, R.L., and Choi, Y. (2021). The DME demethylase regulates sporophyte gene expression, cell proliferation, differentiation, and meristem resurrection. Proc. Natl. Acad. Sci. U. S. A. 118.

33. Köhler, C., Hennig, L., Spillane, C., Pien, S., and Gruissem, W. (2003). The Polycomb -group protein MEDEA regulates seed development by controlling expression of the MADS-box gene *PHERES1*. Genes Dev. 17: 1540–1553.

34. Kuwabara, A. and Gruissem, W. (2014). *Arabidopsis* Retinoblastoma-related and Polycomb group proteins: Cooperation during plant cell differentiation and development. J. Exp. Bot. 65: 2667–2676.

35. Kwon, C.S., Hibara, K.I., Pfluger, J., Bezhani, S., Metha, H., Aida, M., Tasaka, M., and Wagner, D. (2006). A role for chromatin remodeling in regulation of CUC gene expression in the *Arabidopsis* cotyledon boundary. Development 133: 3223–3230.

36. Leroy, O., Hennig, L., Breuninger, H., Laux, T., and Köhler, C. (2007). Polycomb group proteins function in the female gametophyte to determine seed development in plants. Development 134: 3639–3648.

37. Li, H., Handsaker, B., Wysoker, A., Fennell, T., Ruan, J., Homer, N., Marth, G., Abecasis, G., Durbin, R., and 1000 Genome Project Data Processing Subgroup (2009). The Sequence Alignment/Map format and SAMtools. Bioinformatics 25: 2078–2079.

38. Li, W., Liu, H., Cheng, Z.J., Su, Y.H., Han, H.N., Zhang, Y., and Zhang, X.S. (2011). DNA methylation and histone modifications regulate de novo shoot regeneration in *Arabidopsis* by modulating WUSCHEL expression and auxin signaling. PLoS Genet. 7.

39. Lindsey, B.E., Rivero, L., Calhoun, C.S., Grotewold, E., and Brkljacic, J. (2017). Standardized method for high-throughput sterilization of *Arabidopsis* seeds. J. Vis. Exp. 2017: 1–7.

40. Livak, K.J. and Schmittgen, T.D. (2001). Analysis of Relative Gene Expression Data Using Real-Time Quantitative PCR and the 2−ΔΔCT Method. Methods 25: 402–408.

41. Lodha, M., Marco, C.F., and Timmermans, M.C.P. (2013). The ASYMMETRIC LEAVES complex maintains repression of *KNOX* homeobox genes via direct recruitment of Polycomb-repressive complex2. Genes Dev. 27: 596–601.

42. Luo, M., Bilodeau, P., Dennis, E.S., Peacock, W.J., and Chaudhury, a (2000). Expression and parent-of-origin effects for FIS2, MEA, and FIE in the endosperm and embryo of developing *Arabidopsis* seeds. Proc. Natl. Acad. Sci. U. S. A. 97: 10637–10642.

43. Makarevich, G., Villar, C.B.R., Erilova, A., and Köhler, C. (2008). Mechanism of *PHERES1* imprinting in *Arabidopsis*. J. Cell Sci. 121: 906–912.

44. Mayer, K.F.X., Schoof, H., Haecker, A., Lenhard, M., Jürgens, G., and Laux, T. (1998). Role of WUSCHEL in Regulating Stem Cell Fate in the *Arabidopsis* Shoot Meristem. Cell 95: 805–815.

45. Okonechnikov, K., Conesa, A., and García-Alcalde, F. (2016). Qualimap 2: Advanced multi-sample quality control for high-throughput sequencing data. Bioinformatics 32: 292–294.

46. Park, J., Frost, J.M., Park, K., Ohr, H., Tae, G., Kim, S., and Eom, H. (2017). Control of DEMETER DNA demethylase gene transcription in male and fe-

979 male gamete companion cells in *Arabidopsis thaliana*. Proc. Natl. Acad. Sci.
980 U. S. A. 114: 2078–2083.
981
982 47. Pikaard, C.S. and Scheid, O.M. (2014). Epigenetic regulation in plants. Cold
983 Spring Harb. Perspect. Biol. 6: 1–31.
984
985 48. Prasad, K. *et al*. (2011). *Arabidopsis* PLETHORA transcription factors control
986 phyllotaxis. Curr. Biol. 21: 1123–1128.
987
988 49. Qiu, Q., Mei, H., Deng, X., He, K., Wu, B., Yao, Q., Zhang, J., Lu, F., Ma, J.,
989 and Cao, X. (2019). DNA methylation repels targeting of *Arabidopsis* REF6.
990 Nat. Commun. 10: 1–9.
991
992 50. Ramírez, F., Ryan, D.P., Grüning, B., Bhardwaj, V., Kilpert, F., Richter, A.S.,
993 Heyne, S., Dündar, F., and Manke, T. (2016). deepTools2: a next generation
994 web server for deep-sequencing data analysis. Nucleic Acids Res. 44: W160–
995 W165.
996
997 51. Ravi, M. *et al*. (2014). A haploid genetics toolbox for *Arabidopsis thaliana*.
998 Nat. Commun. 5: 5334.
999
1000 52. Ravi, M. and Bondada, R. (2016). Genome Elimination by Tailswap CenH3: In
1001 Vivo Haploid Production in *Arabidopsis thaliana*. Methods Mol Biol. 1469:77-
1002 99.
1003
1004 53. Ravi, M. and Chan, S.W.L. (2010). Haploid plants produced by centromere-
1005 mediated genome elimination. Nature 464: 615–618.
1006
1007 54. Robinson, J.T., Thorvaldsdóttir, H., Winckler, W., Guttman, M., Lander, E.S.,
1008 Getz, G., and Mesirov, J.P. (2011). Integrative genomics viewer. Nat. Bio-
1009 technol. 29: 24–26.
1010
1011 55. Roszak, P.J. and Köhler, C. (2011). Polycomb group proteins are required to
1012 couple seed coat initiation to fertilization. Proc. Natl. Acad. Sci. U. S. A. 108:
1013 20826–20831.
1014
1015 56. Roy, S., Gupta, P., Rajabhoj, M.P., Maruthachalam, R., and Nandi, A.K.
1016 (2018). The polycomb-group repressor MEDEA attenuates pathogen defense.
1017 Plant Physiol.
1018
1019 57. Saleh, A., Al-Abdallat, A., Ndamukong, I., Alvarez-Venegas, R., and
1020 Avramova, Z. (2007). The *Arabidopsis* homologs of trithorax (ATX1) and en-
1021 hancer of zeste (CLF) establish “bivalent chromatin marks” at the silent *AGA*-

MOUS locus. Nucleic Acids Res. 35: 6290–6296.

58. Salvi, E., Rutten, J.P., Di Mambro, R., Polverari, L., Licursi, V., Negri, R., Dello Ioio, R., Sabatini, S., and Ten Tusscher, K. (2020). A Self-Organized PLT/Auxin/ARR-B Network Controls the Dynamics of Root Zonation Development in *Arabidopsis thaliana*. Dev. Cell 53: 431-443.e23.

59. Schmid, M., Davison, T.S., Henz, S.R., Pape, U.J., Demar, M., Vingron, M., Schölkopf, B., Weigel, D., and Lohmann, J.U. (2005). A gene expression map of *Arabidopsis thaliana* development. Nat. Genet. 37: 501–506.

60. Schoft, V.K., Chumak, N., Choi, Y., Hannon, M., Garcia-Aguilar, M., Machlicova, A., Slusarz, L., Mosiolek, M., Park, J.-S., Park, G.T., Fischer, R.L., and Tamaru, H. (2011). Function of the DEMETER DNA glycosylase in the *Arabidopsis thaliana* male gametophyte. Proc Natl Acad Sci USA 108: 8042–7.

61. Schoof, H., Lenhard, M., Haecker, A., Mayer, K.F.X., Jürgens, G., and Laux, T. (2000). The stem cell population of *Arabidopsis* shoot meristems is maintained by a regulatory loop between the *CLAVATA* and *WUSCHEL* genes. Cell 100: 635–644.

62. Schumann, U., Lee, J.M., Smith, N.A., Zhong, C., Zhu, J.K., Dennis, E.S., Millar, A.A., and Wang, M.B. (2019). DEMETER plays a role in DNA demethylation and disease response in somatic tissues of *Arabidopsis*. Epigenetics 14: 1074–1087.

63. Scofield, S., Dewitte, W., and Murray, J.A. (2008). A model for *Arabidopsis* class-1 KNOX gene function. Plant Signal. Behav. 3: 257–259.

64. Shen, W.-H. and Xu, L. (2009). Chromatin Remodeling in Stem Cell Maintenance in *Arabidopsis thaliana*. Mol. Plant 2: 600–609.

65. Simonini, S., Bemer, M., Bencivenga, S., Gagliardini, V., Pires, N.D., Desvoyes, B., van der Graaff, E., Gutierrez, C., and Grossniklaus, U. (2021). The Polycomb group protein MEDEA controls cell proliferation and embryonic patterning in *Arabidopsis*. Dev. Cell 56: 1945-1960.e7.

66. Spillane, C., Schmid, K.J., Laoueillé-Duprat, S., Pien, S., Escobar-Restrepo, J.-M., Baroux, C., Gagliardini, V., Page, D.R., Wolfe, K.H., and Grossniklaus, U. (2007). Positive darwinian selection at the imprinted *MEDEA* locus in plants. Nature 448: 349–352.

67. Spinelli, S.V., Martin, A.P., Viola, I.L., Gonzalez, D.H., and Palatnik, J.F. (2011). A Mechanistic Link between *STM* and *CUC1* during *Arabidopsis* Development. Plant Physiol. 156: 1894–1904.

68. Stahl, Y. and Simon, R. (2010). Plant primary meristems: shared functions and regulatory mechanisms. Curr. Opin. Plant Biol. 13: 53–58.

69. Su, Y.H., Zhou, C., Li, Y.J., Yu, Y., Tang, L.P., Zhang, W.J., Yao, W.J., Huang, R., Laux, T., and Zhang, X.S. (2020). Integration of pluripotency pathways regulates stem cell maintenance in the *Arabidopsis* shoot meristem. Proc. Natl. Acad. Sci. U. S. A. 117: 22561–22571.

70. Sun, B., Looi, L.S., Guo, S., He, Z., Gan, E.S., Huang, J., Xu, Y., Wee, W.Y., and Ito, T. (2014). Timing mechanism dependent on cell division is invoked by Polycomb eviction in plant stem cells. Science 343.

71. Sutherland, E., Coe, L., and Raleigh, E.A. (1992). McrBC: a multisubunit GTP-dependent restriction endonuclease. J. Mol. Biol. 225: 327–348.

72. Ten Hove, C.A., Lu, K.J., and Weijers, D. (2015). Building a plant: Cell fate specification in the early *Arabidopsis* embryo. Development 142: 420–430.

73. Thomas, J., Spillane, C., Coluccio, A., Hoeppner, M.A., and Grossniklaus, U. (1999). Maintenance of genomic imprinting at the *Arabidopsis MEDEA* locus requires zygotic DDM1 activity.: 2971–2982.

74. Varapparambath, V. *et al*. (2022). Mechanical conflict caused by a cell-wall-loosening enzyme activates de novo shoot regeneration. Dev. Cell 57: 2063–2080.

75. Williams, B.P., Bechen, L.L., Pohlmann, D.A., and Gehring, M. (2022). Somatic DNA demethylation generates tissue-specific methylation states and impacts flowering time. Plant Cell 34: 1189–1206.

76. Williams, B.P. and Gehring, M. (2020). Principles of Epigenetic Homeostasis Shared Between Flowering Plants and Mammals. Trends Genet. 36: 751–763.

77. Xiao, J. *et al*. (2017). Cis and trans determinants of epigenetic silencing by Polycomb repressive complex 2 in *Arabidopsis*. Nat. Genet. 49: 1546–1552.

78. Xiao, J., Lee, U.-S., and Wagner, D. (2016). Tug of war: adding and removing histone lysine methylation in *Arabidopsis*. Curr. Opin. Plant Biol. 34: 41–53.

79. Xiao, J. and Wagner, D. (2015). Polycomb repression in the regulation of growth and development in *Arabidopsis*. Curr. Opin. Plant Biol. 23: 15–24.

80. Xiao, W., Gehring, M., Choi, Y., Margossian, L., Pu, H., Harada, J.J., Goldberg, R.B., Pennell, R.I., and Fischer, R.L. (2003). Imprinting of the *MEA* polycomb gene is controlled by antagonism between MET1 methyltransferase and DME glycosylase. Dev. Cell 5: 891–901.

81. Yadav, R.K., Perales, M., Gruel, J., Ohno, C., Heisler, M., Girke, T., Jönsson, H., and Reddy, G.V. (2013). Plant stem cell maintenance involves direct transcriptional repression of differentiation program. Mol. Syst. Biol. 9: 654.

82. Yamaguchi, N., Winter, C.M., Wu, M.-F., Kwon, C.S., William, D.A., and Wagner, D. (2014). PROTOCOL: Chromatin Immunoprecipitation from *Arabidopsis* Tissues. Arab. Book 12: e0170.

83. Yoshida, N., Yanai, Y., Chen, L., Kato, Y., Hiratsuka, J., Miwa, T., Sung, Z.R., and Takahashi, S. (2001). EMBRYONIC FLOWER2, a novel Polycomb group protein homolog, mediates shoot development and flowering in *Arabidopsis*. Plant Cell 13: 2471–2481.

84. Yu, G., Wang, L.G., Han, Y., and He, Q.Y. (2012). ClusterProfiler: An R package for comparing biological themes among gene clusters. OMICS J. Integr. Biol. 16: 284–287.

85. Yu, G., Wang, L.G., and He, Q.Y. (2015). ChIP seeker: An R/Bioconductor package for ChIP peak annotation, comparison and visualization. Bioinformatics 31: 2382–2383.

86. Zhang, H., Tang, K., Wang, B., Duan, C.G., Lang, Z., and Zhu, J.K. (2014). Protocol: A beginner's guide to the analysis of RNA-directed DNA methylation in plants. Plant Methods 10: 1–9.

87. Zhang, S., Wang, D., Zhang, H., Skaggs, M.I., Lloyd, A., Ran, D., An, L., Schumaker, K.S., Drews, G.N., and Yadegari, R. (2018). FERTILIZATION-INDEPENDENT SEED-Polycomb Repressive Complex 2 Plays a Dual Role in Regulating Type I MADS-Box Genes in Early Endosperm Development. Plant Physiol. 177: 285 LP – 299.

88. Zhang, X., Clarenz, O., Cokus, S., Bernatavichute, Y.V., Pellegrini, M., Goodrich, J., and Jacobsen, S.E. (2007). Whole-Genome Analysis of Histone H3 Lysine 27 Trimethylation in *Arabidopsis*. PLOS Biol. 5: e129.

1152 89. Zhang, Y., Liu, T., Meyer, C.A., Eeckhoute, J., Johnson, D.S., Bernstein, B.E.,
1153 Nusbaum, C., Myers, R.M., Brown, M., Li, W., and Liu, X.S. (2008). Model-
1154 based Analysis of ChIP-Seq (MACS). Genome Biol. 9: R137.
1155
1156 90. Zuo, J., Niu, Q.W., and Chua, N.H. (2000). An estrogen receptor-based trans-
1157 activator XVE mediates highly inducible gene expression in transgenic plants.
1158 Plant J. 24: 265–273.

Parsed Citations

Aichinger, E., Villar, C.B.R., Di Mambro, R., Sabatini, S., and Köhler, C. (2011). The CHD3 Chromatin Remodeler PICKLE and Polycomb Group Proteins Antagonistically Regulate Meristem Activity in the Arabidopsis Root. Plant Cell 23: 1047–1060.
Google Scholar: Author Only Title Only Author and Title

Aida, M., Ishida, T., and Tasaka, M. (1999). Shoot apical meristem and cotyledon formation during Arabidopsis embryogenesis: Interaction among the CUP-SHAPED COTYLEDON and SHOOT MERISTEMLESS genes. Development 126: 1563–1570.
Google Scholar: Author Only Title Only Author and Title

Aida, M., Vernoux, T., Furutani, M., Traas, J., and Tasaka, M. (2002). Roles of PIN-FORMED1 and MONOPTEROS in pattern formation of the apical region of the Arabidopsis embryo. Development 129: 3965–3974.
Google Scholar: Author Only Title Only Author and Title

Borg, M., Jacob, Y., Susaki, D. et al. (2020).Targeted reprogramming of H3K27me3 resets epigenetic memory in plant paternal chromatin. Nat Cell Biol 22: 621–629.
Google Scholar: Author Only Title Only Author and Title

Bouyer, D., Kramdi, A., Kassam, M., Heese, M., Schnittger, A., Roudier, F., and Colot, V. (2017). DNA methylation dynamics during early plant life. Genome Biol. 18: 1–12.
Google Scholar: Author Only Title Only Author and Title

Bouyer, D., Roudier, F., Heese, M., Andersen, E.D., Gey, D., Nowack, M.K., Goodrich, J., Renou, J.P., Grini, P.E., Colot, V., and Schnittger, A. (2011). Polycomb repressive complex 2 controls the embryo-to-seedling phase transition. PLoS Genet. 7.
Google Scholar: Author Only Title Only Author and Title

Burian, A., Raczyńska-Szajgin, M., Borowska-Wykręt, D., Piatek, A., Aida, M., and Kwiatkowska, D. (2015). The CUP-SHAPED COTYLEDON2 and 3 genes have a post-meristematic effect on Arabidopsis thaliana phyllotaxis. Ann. Bot. 115: 807–820.
Google Scholar: Author Only Title Only Author and Title

Chaudhury, A.M., Ming, L., Miller, C., Craig, S., Dennis, E.S., and Peacock, W.J. (1997). Fertilization-independent seed development in Arabidopsis thaliana. Proc. Natl. Acad. Sci. U. S. A. 94: 4223–4228.
Google Scholar: Author Only Title Only Author and Title

Chen, D., Molitor, A., Liu, C., and Shen, W.H. (2010). The Arabidopsis PRC1-like ring-finger proteins are necessary for repression of embryonic traits during vegetative growth. Cell Res. 20: 1332–1344.
Google Scholar: Author Only Title Only Author and Title

Choi, Y., Gehring, M., Johnson, L., Hannon, M., Harada, J.J., Goldberg, R.B., Jacobsen, S.E., and Fischer, R.L. (2002). DEMETER, a DNA glycosylase domain protein, is required for endosperm gene imprinting and seed viability in Arabidopsis. Cell 110: 33–42.
Google Scholar: Author Only Title Only Author and Title

Cui, X. et al. (2016). REF6 recognizes a specific DNA sequence to demethylate H3K27me3 and regulate organ boundary formation in Arabidopsis. Nat. Genet. 48: 694–699.
Google Scholar: Author Only Title Only Author and Title

Daimon, Y., Takabe, K., and Tasaka, M. (2003). The CUP-SHAPED COTYLEDON Genes Promote Adventitious Shoot Formation on Calli. Plant Cell Physiol. 44: 113–121.
Google Scholar: Author Only Title Only Author and Title

Dasgupta, P. and Chaudhuri, S. (2019). Analysis of DNA Methylation Profile in Plants by Chop-PCR. In Plant Innate Immunity, W. Gassmann, ed, Methods in Molecular Biology. (Springer New York: New York, NY), pp. 79–90.
Google Scholar: Author Only Title Only Author and Title

De Lucia, F., Crevillen, P., Jones, A.M.E., Greb, T., and Dean, C. (2008). A PHD-polycomb repressive complex 2 triggers the epigenetic silencing of FLC during vernalization. Proc. Natl. Acad. Sci. U. S. A. 105: 16831–16836.
Google Scholar: Author Only Title Only Author and Title

Du, J., Johnson, L.M., Jacobsen, S.E., and Patel, D.J. (2015). DNA methylation pathways and their crosstalk with histone methylation. Nat. Rev. Mol. Cell Biol. 16: 519–532.
Google Scholar: Author Only Title Only Author and Title

Feng, J., Liu, T., Qin, B., Zhang, Y., and Liu, X.S. (2012). Identifying ChIP-seq enrichment using MACS. Nat. Protoc. 7: 1728–1740.
Google Scholar: Author Only Title Only Author and Title

Figueiredo, D.D., Batista, R.A., Roszak, P.J., and Köhler, C. (2015). Auxin production couples endosperm development to fertilization. Nat. Plants 1.
Google Scholar: Author Only Title Only Author and Title

Gehring, M., Bubb, K.L., and Henikoff, S. (2009). Extensive Demethylation of Repetitive Elements During Seed Development

Underlies Gene Imprinting. Science 324: 1447–1451.
Google Scholar: Author Only Title Only Author and Title

Gehring, M., Huh, J.H., Hsieh, T.F., Penterman, J., Choi, Y., Harada, J.J., Goldberg, R.B., and Fischer, R.L. (2006). DEMETER DNA glycosylase establishes MEDEA polycomb gene self-imprinting by allele-specific demethylation. Cell 124: 495–506.
Google Scholar: Author Only Title Only Author and Title

Gong, Z., Morales-Ruiz, T., Ariza, R.R., Roldán-Arjona, T., David, L., and Zhu, J.K. (2002). ROS1, a repressor of transcriptional gene silencing in Arabidopsis, encodes a DNA glycosylase/lyase. Cell 111: 803–814.
Google Scholar: Author Only Title Only Author and Title

Grossniklaus, U., Vielle-Calzada, J.P., Hoeppner, M.A., and Gagliano, W.B. (1998). Maternal control of embryogenesis by MEDEA, a Polycomb group gene in Arabidopsis. Science 280: 446–450.
Google Scholar: Author Only Title Only Author and Title

Guitton, A.-E., Page, D.R., Chambrier, P., Lionnet, C., Faure, J.-E., Grossniklaus, U., and Berger, F. (2004). Identification of new members of Fertilization Independent Seed Polycomb Group pathway involved in the control of seed development in Arabidopsis thaliana. Development 131: 2971–81.
Google Scholar: Author Only Title Only Author and Title

Gutzat, R. et al. (2020). Arabidopsis shoot stem cells display dynamic transcription and DNA methylation patterns. EMBO J. 39.
Google Scholar: Author Only Title Only Author and Title

Heisler, M.G., Ohno, C., Das, P., Sieber, P., Reddy, G.V., Long, J.A., and Meyerowitz, E.M. (2005). Patterns of auxin transport and gene expression during primordium development revealed by live imaging of the Arabidopsis inflorescence meristem. Curr. Biol. 15: 1899–1911.
Google Scholar: Author Only Title Only Author and Title

Higo, A. et al. (2020). DNA methylation is reconfigured at the onset of reproduction in rice shoot apical meristem. Nat. Commun. 11: 1–12.
Google Scholar: Author Only Title Only Author and Title

Hofhuis, H., Laskowski, M., Du, Y., Prasad, K., Grigg, S., Pinon, V., and Scheres, B. (2013). Phyllotaxis and rhizotaxis in Arabidopsis are modified by three plethora transcription factors. Curr. Biol. 23: 956–962.
Google Scholar: Author Only Title Only Author and Title

Ibarra, C.A. et al. (2012). Active DNA Demethylation in Plant Companion Cells Reinforces Transposon Methylation in Gametes. Science 337: 1360–1364.
Google Scholar: Author Only Title Only Author and Title

Iwasaki M and Paszkowski J (2014) Epigenetic memory in plants. EMBO J. 33: 1987-1998.
Google Scholar: Author Only Title Only Author and Title

Kareem, A., Durgaprasad, K., Sugimoto, K., Du, Y., Pulianmackal, A.J., Trivedi, Z.B., Abhayadev, P.V., Pinon, V., Meyerowitz, E.M., Scheres, B., and Prasad, K. (2015). PLETHORA genes control regeneration by a two-step mechanism. Curr. Biol. 25: 1017–1030.
Google Scholar: Author Only Title Only Author and Title

Khouider, S., Borges, F., LeBlanc, C., Ungru, A., Schnittger, A., Martienssen, R., Colot, V., and Bouyer, D. (2021). Male fertility in Arabidopsis requires active DNA demethylation of genes that control pollen tube function. Nat. Commun. 12: 1–10.
Google Scholar: Author Only Title Only Author and Title

Kim, M., Ohr, H., Lee, J.W., Hyun, Y., Fischer, R.L., and Choi, Y. (2008). Temporal and spatial downregulation of Arabidopsis MET1 activity results in global DNA hypomethylation and developmental defects. Mol. Cells 26: 611–615.
Google Scholar: Author Only Title Only Author and Title

Kim, S., Park, J.S., Lee, J., Lee, K.K., Park, O.S., Choi, H.S., Seo, P.J., Cho, H.T., Frost, J.M., Fischer, R.L., and Choi, Y. (2021). The DME demethylase regulates sporophyte gene expression, cell proliferation, differentiation, and meristem resurrection. Proc. Natl. Acad. Sci. U. S. A. 118.
Google Scholar: Author Only Title Only Author and Title

Köhler, C., Hennig, L., Spillane, C., Pien, S., and Gruissem, W. (2003). The Polycomb -group protein MEDEA regulates seed development by controlling expression of the MADS-box gene PHERES1. Genes Dev. 17: 1540–1553.
Google Scholar: Author Only Title Only Author and Title

Kuwabara, A. and Gruissem, W. (2014). Arabidopsis Retinoblastoma-related and Polycomb group proteins: Cooperation during plant cell differentiation and development. J. Exp. Bot. 65: 2667–2676.
Google Scholar: Author Only Title Only Author and Title

Kwon, C.S., Hibara, K.I., Pfluger, J., Bezhani, S., Metha, H., Aida, M., Tasaka, M., and Wagner, D. (2006). A role for chromatin remodeling in regulation of CUC gene expression in the Arabidopsis cotyledon boundary. Development 133: 3223–3230.

Google Scholar: Author Only Title Only Author and Title

Leroy, O., Hennig, L., Breuninger, H., Laux, T., and Köhler, C. (2007). Polycomb group proteins function in the female gametophyte to determine seed development in plants. Development 134: 3639–3648.
Google Scholar: Author Only Title Only Author and Title

Li, H., Handsaker, B., Wysoker, A., Fennell, T., Ruan, J., Homer, N., Marth, G., Abecasis, G., Durbin, R., and 1000 Genome Project Data Processing Subgroup (2009). The Sequence Alignment/Map format and SAMtools. Bioinformatics 25: 2078–2079.
Google Scholar: Author Only Title Only Author and Title

Li, W., Liu, H., Cheng, Z.J., Su, Y.H., Han, H.N., Zhang, Y., and Zhang, X.S. (2011). DNA methylation and histone modifications regulate de novo shoot regeneration in Arabidopsis by modulating WUSCHEL expression and auxin signaling. PLoS Genet. 7.
Google Scholar: Author Only Title Only Author and Title

Lindsey, B.E., Rivero, L., Calhoun, C.S., Grotewold, E., and Brkljacic, J. (2017). Standardized method for high-throughput sterilization of Arabidopsis seeds. J. Vis. Exp. 2017: 1–7.
Google Scholar: Author Only Title Only Author and Title

Livak, K.J. and Schmittgen, T.D. (2001). Analysis of Relative Gene Expression Data Using Real-Time Quantitative PCR and the 2−ΔΔCT Method. Methods 25: 402–408.
Google Scholar: Author Only Title Only Author and Title

Lodha, M., Marco, C.F., and Timmermans, M.C.P. (2013). The ASYMMETRIC LEAVES complex maintains repression of KNOX homeobox genes via direct recruitment of Polycomb-repressive complex2. Genes Dev. 27: 596–601.
Google Scholar: Author Only Title Only Author and Title

Luo, M., Bilodeau, P., Dennis, E.S., Peacock, W.J., and Chaudhury, a (2000). Expression and parent-of-origin effects for FIS2, MEA, and FIE in the endosperm and embryo of developing Arabidopsis seeds. Proc. Natl. Acad. Sci. U. S. A. 97: 10637–10642.
Google Scholar: Author Only Title Only Author and Title

Makarevich, G., Villar, C.B.R., Erilova, A., and Köhler, C. (2008). Mechanism of PHERES1 imprinting in Arabidopsis. J. Cell Sci. 121: 906–912.
Google Scholar: Author Only Title Only Author and Title

Mayer, K.F.X., Schoof, H., Haecker, A., Lenhard, M., Jürgens, G., and Laux, T. (1998). Role of WUSCHEL in Regulating Stem Cell Fate in the Arabidopsis Shoot Meristem. Cell 95: 805–815.
Google Scholar: Author Only Title Only Author and Title

Okonechnikov, K., Conesa, A., and García-Alcalde, F. (2016). Qualimap 2: Advanced multi-sample quality control for high-throughput sequencing data. Bioinformatics 32: 292–294.
Google Scholar: Author Only Title Only Author and Title

Park, J., Frost, J.M., Park, K., Ohr, H., Tae, G., Kim, S., and Eom, H. (2017). Control of DEMETER DNA demethylase gene transcription in male and female gamete companion cells in Arabidopsis thaliana. Proc. Natl. Acad. Sci. U. S. A. 114: 2078–2083.
Google Scholar: Author Only Title Only Author and Title

Pikaard, C.S. and Scheid, O.M. (2014). Epigenetic regulation in plants. Cold Spring Harb. Perspect. Biol. 6: 1–31.
Google Scholar: Author Only Title Only Author and Title

Prasad, K. et al. (2011). Arabidopsis PLETHORA transcription factors control phyllotaxis. Curr. Biol. 21: 1123–1128.
Google Scholar: Author Only Title Only Author and Title

Qiu, Q., Mei, H., Deng, X., He, K., Wu, B., Yao, Q., Zhang, J., Lu, F., Ma, J., and Cao, X. (2019). DNA methylation repels targeting of Arabidopsis REF6. Nat. Commun. 10: 1–9.
Google Scholar: Author Only Title Only Author and Title

Ramírez, F., Ryan, D.P., Grüning, B., Bhardwaj, V., Kilpert, F., Richter, A.S., Heyne, S., Dündar, F., and Manke, T. (2016). deepTools2: a next generation web server for deep-sequencing data analysis. Nucleic Acids Res. 44: W160–W165.
Google Scholar: Author Only Title Only Author and Title

Ravi, M. et al. (2014). A haploid genetics toolbox for Arabidopsis thaliana. Nat. Commun. 5: 5334.
Google Scholar: Author Only Title Only Author and Title

Ravi, M. and Bondada, R. (2016). Genome Elimination by Tailswap CenH3: In Vivo Haploid Production in Arabidopsis thaliana. Methods Mol Biol. 1469:77-99.
Google Scholar: Author Only Title Only Author and Title

Ravi, M. and Chan, S.W.L. (2010). Haploid plants produced by centromere-mediated genome elimination. Nature 464: 615–618.
Google Scholar: Author Only Title Only Author and Title

Robinson, J.T., Thorvaldsdóttir, H., Winckler, W., Guttman, M., Lander, E.S., Getz, G., and Mesirov, J.P. (2011). Integrative

genomics viewer. Nat. Biotechnol. 29: 24–26.
Google Scholar: Author Only Title Only Author and Title

Roszak, P.J. and Köhler, C. (2011). Polycomb group proteins are required to couple seed coat initiation to fertilization. Proc. Natl. Acad. Sci. U. S. A. 108: 20826–20831.
Google Scholar: Author Only Title Only Author and Title

Roy, S., Gupta, P., Rajabhoj, M.P., Maruthachalam, R., and Nandi, A.K. (2018). The polycomb-group repressor MEDEA attenuates pathogen defense. Plant Physiol.
Google Scholar: Author Only Title Only Author and Title

Saleh, A., Al-Abdallat, A., Ndamukong, I., Alvarez-Venegas, R., and Avramova, Z. (2007). The Arabidopsis homologs of trithorax (ATX1) and enhancer of zeste (CLF) establish "bivalent chromatin marks" at the silent AGAMOUS locus. Nucleic Acids Res. 35: 6290–6296.
Google Scholar: Author Only Title Only Author and Title

Salvi, E., Rutten, J.P., Di Mambro, R., Polverari, L., Licursi, V., Negri, R., Dello Ioio, R., Sabatini, S., and Ten Tusscher, K. (2020). A Self-Organized PLT/Auxin/ARR-B Network Controls the Dynamics of Root Zonation Development in Arabidopsis thaliana. Dev. Cell 53: 431-443.e23.
Google Scholar: Author Only Title Only Author and Title

Schmid, M., Davison, T.S., Henz, S.R., Pape, U.J., Demar, M., Vingron, M., Schölkopf, B., Weigel, D., and Lohmann, J.U. (2005). A gene expression map of Arabidopsis thaliana development. Nat. Genet. 37: 501–506.
Google Scholar: Author Only Title Only Author and Title

Schoft, V.K., Chumak, N., Choi, Y., Hannon, M., Garcia-Aguilar, M., Machlicova, A., Slusarz, L., Mosiolek, M., Park, J.-S., Park, G.T., Fischer, R.L., and Tamaru, H. (2011). Function of the DEMETER DNA glycosylase in the Arabidopsis thaliana male gametophyte. Proc Natl Acad Sci USA 108: 8042–7.
Google Scholar: Author Only Title Only Author and Title

Schoof, H., Lenhard, M., Haecker, A., Mayer, K.F.X., Jürgens, G., and Laux, T. (2000). The stem cell population of Arabidopsis shoot meristems is maintained by a regulatory loop between the CLAVATA and WUSCHEL genes. Cell 100: 635–644.
Google Scholar: Author Only Title Only Author and Title

Schumann, U., Lee, J.M., Smith, N.A., Zhong, C., Zhu, J.K., Dennis, E.S., Millar, A.A., and Wang, M.B. (2019). DEMETER plays a role in DNA demethylation and disease response in somatic tissues of Arabidopsis. Epigenetics 14: 1074–1087.
Google Scholar: Author Only Title Only Author and Title

Scofield, S., Dewitte, W., and Murray, J.A. (2008). A model for Arabidopsis class-1 KNOX gene function. Plant Signal. Behav. 3: 257–259.
Google Scholar: Author Only Title Only Author and Title

Shen, W.-H. and Xu, L. (2009). Chromatin Remodeling in Stem Cell Maintenance in Arabidopsis thaliana. Mol. Plant 2: 600–609.
Google Scholar: Author Only Title Only Author and Title

Simonini, S., Bemer, M., Bencivenga, S., Gagliardini, V., Pires, N.D., Desvoyes, B., van der Graaff, E., Gutierrez, C., and Grossniklaus, U. (2021). The Polycomb group protein MEDEA controls cell proliferation and embryonic patterning in Arabidopsis. Dev. Cell 56: 1945-1960.e7.
Google Scholar: Author Only Title Only Author and Title

Spillane, C., Schmid, K.J., Laoueillé-Duprat, S., Pien, S., Escobar-Restrepo, J.-M., Baroux, C., Gagliardini, V., Page, D.R., Wolfe, K.H., and Grossniklaus, U. (2007). Positive darwinian selection at the imprinted MEDEA locus in plants. Nature 448: 349–352.
Google Scholar: Author Only Title Only Author and Title

Spinelli, S.V., Martin, A.P., Viola, I.L., Gonzalez, D.H., and Palatnik, J.F. (2011). A Mechanistic Link between STM and CUC1 during Arabidopsis Development. Plant Physiol. 156: 1894–1904.
Google Scholar: Author Only Title Only Author and Title

Stahl, Y. and Simon, R. (2010). Plant primary meristems: shared functions and regulatory mechanisms. Curr. Opin. Plant Biol. 13: 53–58.
Google Scholar: Author Only Title Only Author and Title

Su, Y.H., Zhou, C., Li, Y.J., Yu, Y., Tang, L.P., Zhang, W.J., Yao, W.J., Huang, R., Laux, T., and Zhang, X.S. (2020). Integration of pluripotency pathways regulates stem cell maintenance in the Arabidopsis shoot meristem. Proc. Natl. Acad. Sci. U. S. A. 117: 22561–22571.
Google Scholar: Author Only Title Only Author and Title

Sun, B., Looi, L.S., Guo, S., He, Z., Gan, E.S., Huang, J., Xu, Y., Wee, W.Y., and Ito, T. (2014). Timing mechanism dependent on cell division is invoked by Polycomb eviction in plant stem cells. Science 343.
Google Scholar: Author Only Title Only Author and Title

Sutherland, E., Coe, L., and Raleigh, E.A. (1992). McrBC: a multisubunit GTP-dependent restriction endonuclease. J. Mol. Biol. 225: 327–348.
Google Scholar: Author Only Title Only Author and Title

Ten Hove, C.A., Lu, K.J., and Weijers, D. (2015). Building a plant: Cell fate specification in the early Arabidopsis embryo. Development 142: 420–430.
Google Scholar: Author Only Title Only Author and Title

Thomas, J., Spillane, C., Coluccio, A., Hoeppner, M.A., and Grossniklaus, U. (1999). Maintenance of genomic imprinting at the Arabidopsis MEDEA locus requires zygotic DDM1 activity.: 2971–2982.
Google Scholar: Author Only Title Only Author and Title

Varapparambath, V. et al. (2022). Mechanical conflict caused by a cell-wall-loosening enzyme activates de novo shoot regeneration. Dev. Cell 57: 2063–2080.
Google Scholar: Author Only Title Only Author and Title

Williams, B.P., Bechen, L.L., Pohlmann, D.A., and Gehring, M. (2022). Somatic DNA demethylation generates tissue-specific methylation states and impacts flowering time. Plant Cell 34: 1189–1206.
Google Scholar: Author Only Title Only Author and Title

Williams, B.P. and Gehring, M. (2020). Principles of Epigenetic Homeostasis Shared Between Flowering Plants and Mammals. Trends Genet. 36: 751–763.
Google Scholar: Author Only Title Only Author and Title

Xiao, J. et al. (2017). Cis and trans determinants of epigenetic silencing by Polycomb repressive complex 2 in Arabidopsis. Nat. Genet. 49: 1546–1552.
Google Scholar: Author Only Title Only Author and Title

Xiao, J., Lee, U.-S., and Wagner, D. (2016). Tug of war: adding and removing histone lysine methylation in Arabidopsis. Curr. Opin. Plant Biol. 34: 41–53.
Google Scholar: Author Only Title Only Author and Title

Xiao, J. and Wagner, D. (2015). Polycomb repression in the regulation of growth and development in Arabidopsis. Curr. Opin. Plant Biol. 23: 15–24.
Google Scholar: Author Only Title Only Author and Title

Xiao, W., Gehring, M., Choi, Y., Margossian, L., Pu, H., Harada, J.J., Goldberg, R.B., Pennell, R.I., and Fischer, R.L. (2003). Imprinting of the MEA polycomb gene is controlled by antagonism between MET1 methyltransferase and DME glycosylase. Dev. Cell 5: 891–901.
Google Scholar: Author Only Title Only Author and Title

Yadav, R.K., Perales, M., Gruel, J., Ohno, C., Heisler, M., Girke, T., Jönsson, H., and Reddy, G.V. (2013). Plant stem cell maintenance involves direct transcriptional repression of differentiation program. Mol. Syst. Biol. 9: 654.
Google Scholar: Author Only Title Only Author and Title

Yamaguchi, N., Winter, C.M., Wu, M.-F., Kwon, C.S., William, D.A., and Wagner, D. (2014). PROTOCOL: Chromatin Immunoprecipitation from Arabidopsis Tissues. Arab. Book 12: e0170.
Google Scholar: Author Only Title Only Author and Title

Yoshida, N., Yanai, Y., Chen, L., Kato, Y., Hiratsuka, J., Miwa, T., Sung, Z.R., and Takahashi, S. (2001). EMBRYONIC FLOWER2, a novel Polycomb group protein homolog, mediates shoot development and flowering in Arabidopsis. Plant Cell 13: 2471–2481.
Google Scholar: Author Only Title Only Author and Title

Yu, G., Wang, L.G., Han, Y., and He, Q.Y. (2012). ClusterProfiler: An R package for comparing biological themes among gene clusters. OMICS J. Integr. Biol. 16: 284–287.
Google Scholar: Author Only Title Only Author and Title

Yu, G., Wang, L.G., and He, Q.Y. (2015). ChIP seeker: An R/Bioconductor package for ChIP peak annotation, comparison and visualization. Bioinformatics 31: 2382–2383.
Google Scholar: Author Only Title Only Author and Title

Zhang, H., Tang, K., Wang, B., Duan, C.G., Lang, Z., and Zhu, J.K. (2014). Protocol: A beginner's guide to the analysis of RNA-directed DNA methylation in plants. Plant Methods 10: 1–9.
Google Scholar: Author Only Title Only Author and Title

Zhang, S., Wang, D., Zhang, H., Skaggs, M.I., Lloyd, A., Ran, D., An, L., Schumaker, K.S., Drews, G.N., and Yadegari, R. (2018). FERTILIZATION-INDEPENDENT SEED-Polycomb Repressive Complex 2 Plays a Dual Role in Regulating Type I MADS-Box Genes in Early Endosperm Development. Plant Physiol. 177: 285 LP – 299.
Google Scholar: Author Only Title Only Author and Title

Zhang, X., Clarenz, O., Cokus, S., Bernatavichute, Y.V., Pellegrini, M., Goodrich, J., and Jacobsen, S.E. (2007). Whole-Genome Analysis of Histone H3 Lysine 27 Trimethylation in Arabidopsis. PLOS Biol. 5: e129.
Google Scholar: Author Only Title Only Author and Title

Zhang, Y., Liu, T., Meyer, C.A., Eeckhoute, J., Johnson, D.S., Bernstein, B.E., Nusbaum, C., Myers, R.M., Brown, M., Li, W., and Liu, X.S. (2008). Model-based Analysis of ChIP-Seq (MACS). Genome Biol. 9: R137.
Google Scholar: Author Only Title Only Author and Title

Zuo, J., Niu, Q.W., and Chua, N.H. (2000). An estrogen receptor-based transactivator XVE mediates highly inducible gene expression in transgenic plants. Plant J. 24: 265–273.
Google Scholar: Author Only Title Only Author and Title